



RESEARCH MEMORANDUM

COMBUSTION OF ALUMINUM BOROHYDRIDE IN A
SUPERSONIC WIND TUNNEL

By Edward A. Fletcher, Robert G. Dorsch, and
Melvin Gerstein

Lewis Flight Propulsion Laboratory
Cleveland, Ohio

NATIONAL ADVISORY COMMITTEE
FOR AERONAUTICS
WASHINGTON

June 20, 1955
Declassified April 15, 1958

NATIONAL ADVISORY COMMITTEE FOR AERONAUTICS

RESEARCH MEMORANDUM

COMBUSTION OF ALUMINUM BOROHYDRIDE IN A SUPERSONIC WIND TUNNEL

By Edward A. Fletcher, Robert G. Dorsch, and Melvin Gerstein

SUMMARY

The feasibility of adding heat to a supersonic airstream in the absence of flameholders was studied. Transient burning for periods of 3 to 10 milliseconds was achieved in a supersonic wind tunnel at nominal Mach numbers of 1.5, 2, 3, and 4. Steady burning was achieved for periods of 0.2 to 2 seconds at nominal Mach numbers of 1.5, 2, and 3. Burning and tunnel flow phenomena, including thermal choking, are described. Possible applications of the results of this study are suggested.

INTRODUCTION

Steady combustion with a high rate of heat release has been the object of much research in connection with turbojet and ram-jet combustion systems. The flow velocities during burning in such combustion chambers are subsonic; and, with conventional fuels, much of the research has had an upper limit of about Mach 0.3 at the combustor inlet. No work is reported of stable burning in a supersonic stream. While a detonation may be considered supersonic burning, a stationary or stabilized detonation has not yet been achieved.

Theoretical studies of heat addition to supersonic flow are reported by a number of authors (refs. 1 to 4). Practical applications of the effect of heat addition on the flow parameters are considered in references 5 to 8. References 5 and 6 describe experiments in which heat is added to the wake of supersonic projectiles. In reference 5 hydrogen was burned at the base of a blunt-base projectile in a Mach 1.6 free jet in order to reduce base drag. The base pressure of a boattailed projectile in free flight at Mach numbers between 1.3 and 2.2 was shown in reference 6 to be increased by the combustion of pyrotechnic powder carried in the base. The effect of external combustion in the neighborhood of a supersonic airfoil on the lift of the airfoil and on the creation of thrust is considered in reference 7. It is proposed that hydrogen be burned subsonically behind a normal shock, the flame being stabilized with flameholders. One important disadvantage of this method is the increase in drag that would be caused by the presence of flameholders on

the wing. Reference 8 shows theoretically that the lift coefficient and the lift-drag ratio are significantly increased if heat is added directly to the supersonic stream under the airfoil.

These references indicate that external combustion in portions of a supersonic stream about an airfoil or body of revolution can reduce drag, improve lift, and create thrust. Thus, external combustion might be a valuable adjunct to a conventional propulsion system, since it would provide the equivalent of an additional source of power for supersonic acceleration or climb without increasing engine size in order to provide reserve thrust.

The addition of heat to a supersonic stream has heretofore been considered impractical because of the difficulty of stabilizing a flame front. Therefore, a preliminary investigation was undertaken at the NACA Lewis laboratory to study the feasibility of adding heat to a supersonic airstream in the vicinity of an airfoil by combustion in the absence of any disturbances except those caused by the airfoil and by the combustion itself. The goal of the investigation was combustion of a type that would permit further aerodynamic studies to be made on the effect of heat addition. Aluminum borohydride was chosen as the fuel, because previous experience has shown that it ignites readily in air even under extreme conditions of low temperature and pressure (e.g., see ref. 9, which also gives pertinent physical and chemical properties).

This report outlines the techniques used to obtain combustion in a supersonic wind tunnel and describes qualitatively the effects observed. Schlieren and direct photographic studies of both transient and steady-state combustion of aluminum borohydride and the attendant wind-tunnel flow changes were made at tunnel Mach numbers of 1.5, 2, and 3. In addition, transient studies were made at Mach 4. The transient runs were essentially exploratory and served to guide subsequent work with steady heat addition.

APPARATUS AND PROCEDURE

The experimental setup consisted of the wind tunnel, photographic equipment, fuel-injection system, and ignition system arranged as shown schematically in figure 1(a).

Wind Tunnel

The combustion of aluminum borohydride injected into the tunnel airstream adjacent to the tunnel wall was studied in a 3.84- by 10-inch supersonic wind tunnel having 1-inch-thick plate-glass sides. The windows ran the entire length of the tunnel down to the subsonic diffuser (fig. 1(b)), permitting convenient visual observation and picture-taking.

Tunnel stagnation pressures ranged from 37 to 50 inches of mercury. The tunnel air had a nominal dewpoint of -20° F and was preheated to 80° to 110° F. Typical test-section conditions are listed in table I.

A boundary-layer study made in this tunnel at Mach 2 (ref. 10) indicates that the boundary-layer flow at the point of fuel injection is as shown in figure 2(a). Several total-pressure surveys made during the present investigation agreed with these data. Figure 2(b) shows the thickness of the boundary layer as a function of the distance downstream of the throat. A two-couple iron-constantan (30-gage) thermocouple rake 33 inches downstream of the injector measured temperature in some of the runs. For hotter regions closer to the injector, chromel-alumel thermocouples were used.

Photography

High-speed (1000 to 4000 frames per sec) direct motion pictures were taken of the flames. Simultaneously, high-speed schlieren motion pictures of a portion of the test section were taken. In addition, an 8- by 10-inch still camera provided open-shutter pictures giving an integrated picture of the entire zone of visible combustion. Because plate-glass walls were used instead of optical glass, the schlieren pictures contain a large number of fixed striations. However, the main shock-wave formations could be ascertained satisfactorily in spite of the apparent density-gradient patterns of the glass.

Fuel Injection

Aluminum borohydride was injected into the airstream by two different techniques. Flow rates of the order of 100 cc per second (55 g/sec) were used for short intervals (3 to 8 millisecc) to observe transient phenomena associated with a high rate of heat addition. Lower fuel-flow rates of the order of 3 cc per second (1.7 g/sec) were used to obtain a steady state (up to 2 sec) with more moderate heat addition. Inasmuch as the tunnel had a small cross section and the walls were glass, it seemed inadvisable to inject at a high fuel-flow rate for longer periods of time.

Transient combustion. - Rapid injections of fuel were made from glass capsules (fig. 3) containing $1/2$ to 1 cc of liquid aluminum borohydride and enough dry nitrogen to bring the pressure within the capsule up to about $1\frac{1}{2}$ atmospheres at room temperature. The capsules were filled by conventional vacuum-transfer techniques and sealed off. During injection the capsule was held in place by the holder mounted on the centerline of the top wall near the upstream end of the wind-tunnel section (fig. 3(b)). After flow in the tunnel had become steady, the scored

tip of the capsule was broken off by a remotely controlled striker. The extension of the end of the barrel of the capsule holder from the top wall of the tunnel could be varied from zero to about 1 inch. Schlieren motion pictures of the injection pattern of the liquid aluminum borohydride as it is expelled from a capsule into the test section of the Mach 4 tunnel are shown in figure 4. The aluminum borohydride shows up as a dark area (combustion has not yet started in this series of pictures). This figure shows that the liquid penetrates well out into the stream and that the fuel jet is thoroughly shattered by the impact of the supersonic stream. In addition, the figure shows that during the injection period the liquid modifies the three-dimensional shock structure caused by the injector.

Steady-state combustion. - Slower, longer, steady-state injections were made with the valve-type injector illustrated in figure 5. This injector was charged, usually with 5 cc of aluminum borohydride, through the upper valve by distillation to the filling arm from a conventional vacuum line. It was then mounted flush with the top wall of the tunnel (to minimize flow disturbances) and pressurized with helium through the upper filling valve. After steady flow had been achieved in the tunnel, the lower valve was opened remotely by the motor driven chain-drive mechanism, and the liquid was sprayed into the tunnel. A considerable variation in flow rate could be achieved by varying the helium pressure between 7.5 and 38 pounds per square inch gage and by varying the fuel orifice size from 1/64 to 3/64 inch in diameter. The interchangeable orifices are shown in figure 5. The duration of these injections varied from 1 to 3 seconds.

Equivalence ratios associated with the different modes of injection at the various Mach numbers are given in table II. These ratios are calculated with the assumption that the fuel is completely mixed with the air flowing through the upper third of the tunnel. Flame usually filled this region. These ratios should serve only to indicate trends and orders of magnitude.

Ignition

Although the material ejected from capsules usually ignited spontaneously, it was found desirable to introduce either an ignitor capsule or a spark plug to ensure ignition in some of the steady-state runs. The ignitor capsule was simply one of the capsules described previously, which was mounted in the center of the top wall of the tunnel (fig. 1) 25 inches downstream of the point of injection. It was broken shortly after the valve on the steady injector had been opened. When flow conditions rendered ignition even more difficult, the ignitor capsule was replaced by a 1-joule, 5-spark-per-second repeating capacitance spark. After ignition the flame quickly traveled upstream to the point of injection and remained seated there until the fuel was expended.

RESULTS AND DISCUSSION

Transient Runs

A summary of the 42 transient runs at Mach numbers of 1.5, 2, 3, and 4 is presented in table III. Included in the table are a description of the intensity of burning and the extension of the injector barrel below the top wall of the tunnel.

Flame usually appeared as a momentary, very intense, bright green flash and was frequently accompanied by a distinct loud bang that could be clearly heard above the tunnel noise. The greater part of the combustion took place within a period of about 3 to 8 milliseconds, but there were frequently secondary flashes that presumably resulted from the dripping of small amounts of aluminum borohydride from the walls of the capsule. Occasionally there were less vigorous runs where it appeared that the main body of the fuel had not ignited. In these runs the flame was weak and pale blue. Many of the burnings, however, took place with explosive violence, frequently completely choking the tunnel and driving the flame at very high speed a considerable distance upstream of the point of injection, sometimes almost back to the tunnel throat. No clearly defined structural details such as a distinctive flame front could be discerned either in the direct or schlieren photographs. The photographs that follow were selected to illustrate some of the phenomena observed and are not unique for any particular Mach number or injector position.

A Mach 1.5 capsule run is illustrated in figure 6 (run 37 in table III). In this run, the capsule-breaking device was mounted so that the end of the barrel was flush with the top wall of the tunnel. Thus, only the end of the capsule and the striking lever projected into the stream. The burning illustrated in this figure resulted from the injection of $1/2$ cubic centimeter of fuel and was considered very strong, but not explosively violent.

Direct motion pictures (3333 frames per sec) of the flame are shown in figure 6(a). Schlieren motion pictures (3348 frames per sec), which were taken simultaneously with the direct motion pictures, are shown in figure 6(b). The schlieren system was centered approximately at the point of injection. Both sets of pictures are matched with an arbitrary time base in which zero time was approximately 1.6 milliseconds before the first appearance of flame. The time on this base is indicated beside each frame. Thus, direct and schlieren pictures having the same time coordinate may be considered simultaneous.

Some idea of the intensity of the flame may be obtained from the direct photographs (fig. 6(a)). In spite of the very short exposure time (10^{-4} sec at $f/2.3$) the film (contrast orthochromatic with an equivalent

speed of ASA 160) was highly overexposed. These pictures show that ignition took place very close to the point of injection at 1.65 milliseconds. At 1.95 milliseconds the luminous region is quite long; but 0.3 millisecond later (at 2.25 millisecond), it has shrunk - that is, the downstream edge has traveled upstream. Subsequently, the downstream end of the luminous region quickly traveled downstream. The second time flame traveled downstream (from 2.25 to 3.45 millisecond), it was traveling in a region where there had just previously been no unburned fuel for flame propagation. That is to say, the flame observed in this region in the interval from 2.25 to 3.45 milliseconds resulted from the transport of either flame or fuel from a region farther upstream. The rate at which the luminous zone traveled downstream should thus serve to permit an estimate of the minimum velocity in this part of the tunnel in this interval. This average velocity in frames 3, 4, and 5 is of the order of 1400 feet per second, which is the undisturbed stream velocity in the tunnel test section. Thus, during this interval at least, the stream velocity apparently had not changed.

The behavior of the flow during the run is shown in the schlieren photographs of figure 6(b). In frame 1, the average Mach number is 1.45 ahead of the shock wave off the injector and is about 1.42 in the region behind the shock. Frames 1 to 4 show the action in the tunnel during breaking of the capsule. In frame 4 (1.64 millisecond), unburned liquid fuel can be seen downstream of the point of injection and, in fact, obscures the tip of the capsule. In frame 5, ignition has already taken place and the shock wave has already traveled upstream about $\frac{1}{2}$ inches. Frames 6 to 10 show the flame, accompanied by the shock wave, going upstream at a speed of about 220 feet per second with respect to the tunnel. As the flame advances, a decided steepening of the shock system occurs between frames 8 and 14 as more heat is added to this region of the stream, indicating that thermal choking is beginning to occur. By frame 27 (8.51 millisecond), the tunnel is choked. That is, the average flow velocity in this region has been driven close to sonic. In frame 71 (21.66 millisecond), the normal shock of the tunnel is beginning to move back downstream again as the combustion is dying out in this area. The normal shock has moved back downstream as far as the capsule holder by frame 104 (31.51 millisecond), and supersonic flow is completely reestablished in this area by frame 200 (60.19 millisecond). This sequence of schlieren photographs is a clear-cut illustration of the phenomenon of thermal choking and subsequent reestablishment of supersonic flow.

In summary, it appears that the burning shown in figure 6 started about 1 millisecond after the start of the fuel injection and continued quite vigorously for about 8 milliseconds. By this time the main body of the fuel had been used up, but dribblets from the capsule continued to burn for about 34 milliseconds more. The shock wave initially off the end of the capsule started moving upstream when combustion started, moving

400 feet per second for about 0.6 millisecond and then slowing down to a fairly constant 220 feet per second. Choking of the tunnel was virtually complete at about 3 milliseconds, after about three-fourths of the vigorous burning had been completed. Restoration of normal flow in the tunnel was quite slow. The normal shock did not return to the injector position until about 20 milliseconds after completion of the vigorous burning, and normal flow was not established in this section of the tunnel for an additional 20 milliseconds, at about the same time that the last dribblets of fuel from the capsule had stopped burning. Figure 7 is an integrated open-shutter photograph of this run.

Ignition at Mach 3 was more difficult than at the other Mach numbers. Of a total of twelve capsule injections, only seven ignited (table III). In this tunnel, optimum flow existed at Mach 3; there were few stray shock waves, and the axial static-pressure profile was quite smooth. The absence of these disturbances may make the spontaneous ignition of aluminum borohydride more difficult. This view is supported by the observation that of nine capsule injections made with the barrel of the injector flush with the top wall of the tunnel to minimize disturbances, only four ignited. With the barrel of the injector inserted $3/4$ inch into the tunnel to generate a stronger shock and increase flow disturbances, three injections ignited and there were no failures. It should, of course, be kept in mind that insertion of the injector barrel into the stream may have served to bring about better atomization and mixing of the fuel, since the observations do not rule out this mechanism for improving the ignition characteristics. In general, the point at which ignition took place varied from run to run and did not appear to be related either to the Mach number or the injector position.

Transient combustion of $1/2$ -cc aluminum borohydride at Mach 3 (run 25 of table III) is illustrated in figure 8. Comparison of the schlieren and direct motion pictures of this run reveals that most of the fuel was ejected and traveled unburned downstream apparently all the way to the diffuser, where ignition took place. Flame then either propagated upstream near the top wall of the tunnel back into the test section or was blown back upstream in the upper portion of the tunnel by the explosion in the diffuser. Burning then continued near the point of injection for about 7 to 10 milliseconds and died out gradually. The flashback velocities in frames 2, 3, 4, 5, and 6 of figure 8(a) are, respectively, about 1400, 1250, 1100, 950, and 800 feet per second, with respect to the tunnel; that is, either mass transfer or flame propagation was supersonic upstream during at least part of the run. The schlieren photographs show no evidence of tunnel choking.

All seven capsule injections at Mach 4 resulted in ignition. Of these, three were explosively violent and four were weak. There seemed to be no correlation between the depth of insertion of the capsule holder and the violence of the combustion. Figure 9 shows an explosively violent

run photographed at 2700 frames per second, at Mach 4 (run 16 of table III). Figure 10 is the open-shutter picture of the same run. Note that flame advanced upstream almost to the throat of the tunnel.

In addition to the capsule runs described in table III, four special runs were made at Mach 3 in which 1/2-cc aluminum borohydride was injected from capsules equipped with capillary tubes to simulate the fuel-flow rates of the steady-state runs that followed. The fuel-oxidant ratio was thus about 1/40 of that in the other capsule runs. Three of these capsules were mounted in the "flush" position and one with the injector barrel 3/4 inch into the tunnel. No ignition resulted.

Only very gross behavior can be predicted with any degree of certainty in the runs previously described. Their violence and highly transient nature precluded any sort of precise observation or measurement.

Steady-State Runs

Since the object of the present research was to establish the feasibility of achieving a sort of heat addition that might be useful in the study of aerodynamic problems and the propulsion of aircraft, the study was extended in an attempt to achieve supersonic burning in the steady state. Since prolonged high temperatures might have a very dangerous effect on the glass tunnel walls, the steady-state runs were made with much lower fuel-flow rates.

The results of all attempted steady-state runs are summarized in table IV. Successful steady-state burning was attempted and achieved at tunnel design Mach numbers of 1.5, 2, and 3. As with the capsule runs, ignition was most difficult at Mach 3. This fact is illustrated in table V, which summarizes the ignition behavior in the steady-state runs as well as the transient runs. As tunnel conditions were changed from Mach 1.5 to 2 to 3, tunnel flow became smoother, and ignition became more difficult. At Mach 2, spontaneous ignition could not be relied upon in the steady-state runs, but the capsule source was a dependable ignitor. At Mach 3, capsules could no longer be used for ignition, but the spark ignition system proved adequate. No steady runs were attempted at Mach 4. Therefore, the available data do not show whether ease of ignition was at a minimum at Mach 3 or whether ignition was becoming more difficult as the Mach number increased.

Some of the phenomena observed in steady-state runs at Mach 2 may be illustrated by runs 7 and 11 of table IV. Portions of run 7 are shown in figure 11. High-speed motion pictures of the combustion of 7 cc of aluminum borohydride in the Mach 2 wind tunnel are shown in figure 11(a). The method of indicating times is the same as that used previously. In this run, there was no external source of ignition; that is, the valve on

the injector was merely opened to allow aluminum borohydride to spray into the tunnel, where it ignited spontaneously after some delay at a point downstream of the injector, flashed back to the injector region, and continued to burn smoothly. From the direct motion pictures, the flashback velocities with respect to the tunnel can be estimated; and in frames 2, 3, and 4 they are approximately 1000, 2100, and 3200 feet per second, respectively. If the stream through which the flame was propagating was flowing against the flame, the spatial flame velocities in the gas were, of course, much higher.

Flame velocities of this magnitude are usually associated with detonation waves, yet examination of the schlieren photographs taken simultaneously (fig. 11(b)) reveals no evidence that the flame front is associated with a shock wave. In this sequence the center of the schlieren system was located about 17 inches downstream of the point of injection. The first four frames show the tunnel with fuel streaming down the test section (the more darkly shaded region just below the top wall of the tunnel) before ignition. The reflected shock wave extending from the lower right-hand corner to the upper left was not present initially, but appeared as the valve admitting aluminum borohydride to the test section was opened. It is therefore attributed to the disturbance caused by the injection of liquid. Ignition has already taken place by frame 5 but has not yet reached the position covered by the schlieren system. Flame has already reached this section in frame 6, and is moving rapidly upstream; by frame 7, about 0.4 millisecond later, the flame front has moved all the way out of view of the schlieren system, corresponding to a minimum (and very conservative) flashback velocity estimate of 1550 feet per second with respect to the tunnel.

In run 11 (fig. 12), the flashback velocities were estimated from the films to be quite low compared with those of run 7. Yet the flame front was accompanied by a shock wave. The ultimate flashback velocity in this run - that is, the velocity with respect to the tunnel at the time when the flame front reached the injector - was about 990 feet per second, considerably lower than that in the previously described run.

Spark-plug ignition proved to be reliable at Mach 3. Combustion was quite smooth and easy to maintain. After burning started at the spark plug, flame quickly traveled upstream and remained seated near the point of injection until the fuel was exhausted. Such a Mach 3 run is illustrated in figure 13 (run 18 of table IV). The flashback velocity ranged from about 300 feet per second near the spark plug to about 700 feet per second at the upstream end of the flame travel. The schlieren photographs (fig. 13(b)) illustrate ignition at the spark plug and show at first a rather large dark region (unignited fuel) extending about 2 to 3 inches down into the tunnel. Frames 1 and 2 show a weak shock associated with the spark-plug electrodes. Identification of this shock is easier if reference is first made to frame 3, where the position of

the electrodes can be determined. By frame 3, ignition has already taken place and flame has started propagating upstream, accompanied by a fairly strong shock wave that stays with the flame front and persists until the end of the run.

The temperatures achieved in the combustion region were of the order of 2500° to 3500° F about 14 inches downstream of the point of injection and about 1 inch from the top wall. Farther downstream, 33 inches from the point of injection, temperatures of 650° and 1100° F were recorded 1/8 and 1 1/8 inches from the top wall of the tunnel.

The time-averaged distribution of luminosity associated with burning and heat addition at Mach 2 is shown in figure 14 (run 13 of table IV). Because of its inertia, an airfoil should experience an over-all pressure variation that could be attributed to the time-averaged distribution of flame shown in figure 14. That is, the transient fluctuations of the flame observed in the high-speed motion pictures would be expected to be relatively unimportant. The wing would feel only the over-all effect.

Ash patterns formed on the top wall of the tunnel were quite similar in all of the runs, usually differing only in the amount of ash deposited. The patterns indicated that burning usually took place in a region covering 75 percent or more of the spanwise dimension of the tunnel. An ash pattern from a Mach 3 run is illustrated in figure 15. This ash deposit was somewhat heavier than usual but was chosen because it clearly illustrates the pattern.

General Discussion

There can be little doubt that flow in the tunnel was supersonic before the commencement of burning in all of the runs, both transient and steady. Furthermore, although the tunnel appeared to be choked in some of the more violent transient runs, in many of the transient runs and in all of the steady runs flow through most of the tunnel cross section continued supersonic, even though vigorous burning lasted for several seconds. It thus appears that, at least after ignition had taken place, an exothermic chemical reaction was stabilized in the absence of flameholders in a region that was supersonic in the absence of combustion.

In all the runs, much burning took place in regions considerably outside the original limits of the boundary layer. At Mach 2 the boundary layer was 0.5 inch thick at the upstream end of the test section and about 1.0 inch thick at the downstream end. At the position of the fuel injector, the boundary layer was 0.6 inch thick and the ratio of boundary-layer velocity to free-stream velocity was greater than 0.5 for distances

from the wall greater than 0.01 inch. However, it is uncertain what part, if any, the boundary layer may have played in the stabilization of the flame. In addition, since heat addition tends to drive both supersonic and subsonic streams toward Mach 1, it is expected that the characteristics of the boundary layer would be changed considerably during combustion.

Three combustion phenomena took place in the tests: ignition, propagation of flame to the fuel-injection region, and steady burning. The probability of spontaneous ignition, it appears, was a function of fuel-air ratio. Thus, at the two conditions where sufficient numbers of attempted runs were made to allow a rough comparison (Mach 2 and 3), ignition was most likely to take place where the fuel-flow rate was high. At Mach 2 all injections ignited spontaneously when the fuel-flow rate was 55 grams per second and the equivalence ratio (ϕ) was estimated to be 0.38 in the upper third of the tunnel. At a fuel-flow rate of 1.7 grams per second ($\phi \approx 0.012$), only one out of six runs ignited spontaneously. At Mach 3 at the higher fuel-flow rate ($\phi \approx 1$), seven out of twelve of the charges ignited spontaneously; while, at the lower flow rate ($\phi \approx 0.03$), none of nine trials ignited. This was perhaps to be expected and merely indicates that under the conditions of the experiment there is some lean limit to spontaneous ignition. The extreme violence of combustion associated with those Mach 4 runs that ignited early during the injection period can probably be attributed to the high local equivalence ratio, 2.3.

That smoothness of tunnel flow may also be of importance in ignition is indicated in table V. Regardless of the fuel-flow rate, spontaneous ignition was least likely at Mach 3 where tunnel flow was smoothest. Disturbing the flow at Mach 3 apparently increased the likelihood of spontaneous ignition; of the seven successful capsule runs at Mach 3, three occurred with the barrel of the capsule holder projecting into the stream, while all five of the failures occurred with the barrel flush with the top wall of the tunnel. The utility of shocks in igniting the mixtures was further indicated by the observation that many of the ignitions occurred in the diffuser. This is in accord with the reports of several observers (refs. 11 to 13) of ignitions in other systems. It should be kept in mind, however, that more effective mixing of fuel and air when the injector barrel was far into the stream may also have been a factor facilitating spontaneous ignition.

In any event, ignition should present no serious problem in the study of steady-state burning, since it could be readily brought about even at the most severe conditions of tunnel flow and equivalence ratio employed in these studies merely by the use of suitable igniting charges or sparks.

The second and third steps of the combustion, propagation to the region of injection and steady burning from the region of injection, always

occurred smoothly. For this reason no study was made of the various parameters other than Mach number that may have affected these phenomena.

Several other observations are not as yet definitely explained. For example, in some of the capsule runs flame moved upstream far beyond the point of injection at high velocities comparable to detonation velocities. It is possible that detonations in the tunnel or diffuser actually reversed a portion of the tunnel flow momentarily and carried unburned fuel and/or the products of combustion upstream. This effect was most noticeable in the very fuel-rich Mach 4 runs.

Nor were the steady-state runs without their apparent inconsistencies. The authors can give no explanation other than the possible inadequacy of the photographic technique for the absence of a shock wave in run 7 (fig. 11), where the velocity of upstream propagation was several thousand feet per second with respect to the tunnel, and the presence of a shock wave in run 11 (fig. 12) where the upstream propagation velocity was less than 1000 feet per second.

CONCLUDING REMARKS

The present investigation has shown that ignition and combustion of aluminum borohydride can be achieved in a supersonic wind tunnel. Steady burning was achieved in the absence of a flameholder, and heat was added to a supersonic airstream without otherwise disturbing the flow. These results suggest that the combustion of aluminum borohydride may be useful in the study of the effect of heat addition on supersonic flow.

At tunnel conditions, the low static temperatures present a more severe ignition problem than would be expected in a practical flight application. On the other hand, the static pressures at which stable burning was achieved in the tunnel correspond to conditions of flight at altitudes of current interest. It is therefore quite reasonable to conclude that aluminum borohydride or similar fuels - for example, pentaborane or the alkylboranes - may have practical application in external heat addition in the vicinity of airfoils to provide an acceleration assist at supersonic speeds.

In addition to this possible application, the results suggest that the use of aluminum borohydride or similar fuels might be expected to increase greatly the maximum permissible flow velocity through thermal-jet engines. Such fuels might be expected to overcome some of the limitations imposed by fuels having lower flame speeds, blow-out limits, and rates of heat release.

Finally, the results offer further substantiation to the suggestion of reference 14 that aluminum borohydride offers a possible means of

reestablishing combustion in a thermal-jet engine after flame-out has occurred and combustor conditions have dropped below the burning limit.

Lewis Flight Propulsion Laboratory
National Advisory Committee for Aeronautics
Cleveland, Ohio, April 12, 1955

REFERENCES

1. Hicks, Bruce L., Montgomery, Donald J., and Wasserman, Robert H.: On the One-Dimensional Theory of Steady Compressible Fluid Flow in Ducts with Friction and Heat Addition. *Jour. Appl. Phys.*, vol. 18, no. 10, Oct. 1947, pp. 891-903.
2. Shapiro, Ascher H., and Hawthorne, W. R.: The Mechanics and Thermodynamics of Steady One-Dimensional Gas Flow. *Jour. Appl. Mech.*, vol. 14, no. 4, Dec. 1947, pp. A317-A336.
3. Tsien, H. S., and Beilock, Milton: Heat Source in a Uniform Flow. *Jour. Aero. Sci.* vol. 16, no. 12, Dec. 1949, p. 756.
4. Pinkel, I. Irving, and Serafini, John S.: Graphical Method for Obtaining Flow Field in Two-Dimensional Supersonic Stream to Which Heat is Added. NACA TN 2206, 1950.
5. Baker, W. T., Davis, T., and Matthews, S. E.: Reduction of Drag of a Projectile in a Supersonic Stream by the Combustion of Hydrogen in the Turbulent Wake. CM-673, *Appl. Phys. Lab.*, The Johns Hopkins Univ., June 4, 1951. (Contract NOrd 7386, with Bur. Ord., U. S. Navy.)
6. Scanland, T. S., and Hebrank, W. H.: Drag Reduction Through Heat Addition to the Wake of Supersonic Missiles. Memo. Rep. 596, *Ballistic Res. Labs.*, Aberdeen Proving Ground (Md.), June 1952. (Proj. No. TB3-0110, Res. and Dev. Div., Ord. Corps.)
7. Smith, E. H., and Davis, T.: The Creation of Thrust and Lift by Combustion on External Surfaces of Aerofoils. *Bur. Ord.*, Dept. Navy, Sept. 1, 1952. (NOrd 12141.)
8. Pinkel, I. Irving, Serafini, John S., and Gregg, John L.: Pressure Distribution and Aerodynamic Coefficients Associated with Heat Addition to Supersonic Air Stream Adjacent to Two-Dimensional Supersonic Wing. NACA RM E51K26, 1952.

9. Straight, David M., Fletcher, Edward A., and Foster, Hampton H.: Aluminum Borohydride as an Ignition Source for Turbojet Combustors. NACA RM E53G15, 1953.
10. Brinich, Paul F.: Boundary-Layer Measurements in 3.84- by 10-Inch Supersonic Channel. NACA TN 2203, 1950.
11. Steinberg, M., and Kaskan, W. E.: The Ignition of Combustible Mixtures by Shock Waves. Paper No. 67, Fifth Symposium (International) on Combustion, The Univ. of Pitts., 1954, p. 140.
12. Shepherd, W. C. F.: The Ignition of Gas Mixtures by Impulsive Pressures. Third Symposium on Combustion and Flame and Explosion Phenomena, The Williams & Wilkins Co. (Baltimore), 1949, pp. 301-316.
13. Fay, James A.: Some Experiments on the Initiation of Detonation in $2H_2-O_2$ Mixtures by Uniform Shock Waves. Fourth Symposium (International) on Combustion, The Williams & Wilkins Co. (Baltimore), 1953, pp. 501-507.
14. Foster, Hampton H., Fletcher, Edward A., and Straight, David M.: Aluminum Borohydride - Hydrocarbon Mixtures as a Source of Ignition for a Turbojet Combustor. NACA RM E54K12, 1955.

TABLE I. - TYPICAL TEST-SECTION CONDITIONS ASSOCIATED WITH VARIOUS MACH NUMBERS IN THE 3.84- BY 10-INCH SUPERSONIC WIND TUNNEL

Mach number	Static pressure, in. Hg	Static temperature, $^{\circ}\text{F}$	Linear flow velocity, ft/sec	Quality of flow
1.5	12	-74	1443	Fair; static-pressure profile irregular; large number of shock waves present
2	5.6	-148	1727	Good; static-pressure profile less irregular; fewer shocks present
3	1.3	-260	2082	Excellent; fairly flat static-pressure profile; few disturbances
4	0.3	-327	2270	Poor; flow slightly unstable; pressure profile irregular

TABLE II. - REPRESENTATIVE FUEL-AIR EQUIVALENCE RATIOS AT VARIOUS MACH NUMBERS^a

Mach number	Air flow through entire cross section, g/sec	Equivalence ratio, ϕ	
		Transient injection	Steady injection
1.5	6311	0.30	0.0094
2	5039	0.38	0.012
3	2075	0.91	0.028
4	835	2.28	

^aThe equivalence ratios are calculated assuming that the fuel is mixed with the air flowing through the upper third of the tunnel.

TABLE III. - TRANSIENT COMBUSTION RUNS

Run	Volume of aluminum borohydride, cc	Depth of insertion of injector, in.	Vigor of burning	Sound accompanying burning	Appearance of flame	
Mach number, 1.5						
31 33 35 ^a 37	1/2	0	Weak	None	Mild flash	
			Moderate	Mild bang	Moderate green flash	
			Explosively violent	Mild bang	Very bright flash	
			Very strong	Mild bang	Moderate blue-green flash	
6 9 10		1/4	Explosively violent	Very weak	None	Bright green flash
				Weak	None	Very pale small flash
				Weak	None	Mild flash
38		3/4	Explosively violent	Weak	Loud bang	Bright green flash
3				Explosively violent	None	Bright green flash
7					Loud bang	Bright green flash
8	1	0	Explosively violent	Loud bang	Bright green flash	
4			Explosively violent	None	Bright green flash went about 1 foot upstream of injector	
30				Very loud bang	Very intense bright green flash	
32				Very strong	Loud bang	Very bright flash
34				Very strong	None	Very bright flash
36				Explosively violent	Loud bang	Intense blue-green flash
5 1 and 2				1/4 3/4	Explosively violent Weak	Loud bang None
Mach number, 2						
39 40 and 41 42	1/2	0	Moderate Very strong Moderate	Mild bang Loud bang Loud bang	Green flame Bright green flame Bright green flame	
Mach number, 3						
19, 23, 26, 27, and 29 20 and 28	1/2	0	----- Very strong	----- Loud bang	No burning Very intense bright green flash	
24 and ^b 25			Moderate	Loud bang	Bright green flash	
18 21 22		3/4	Explosively violent	Weak	Loud bang	Green flash
	Weak			Loud bang	Very intense bright green flash	
	Weak			Loud bang	Pale blue-green flash	
Mach number, 4						
15 13 and 14 11 and 12	1/2	0	Weak	Mild bang	Small bluish flame	
		3/8	Weak	Mild bang	Small bluish flame	
		1/2	Explosively violent	Loud bang	Entire test section seemed to fill with bright green flame	
^c 16	7/8	Explosively violent	Explosively violent	Very loud bang	Very bright green flash backed all the way up into nozzle	
17			Weak	Mild bang	Weak bluish flame	

^aIllustrated in figures 6 and 7.^bIllustrated in figure 8.^cIllustrated in figures 4, 9, and 10.

TABLE IV. - STEADY-STATE COMBUSTION RUNS

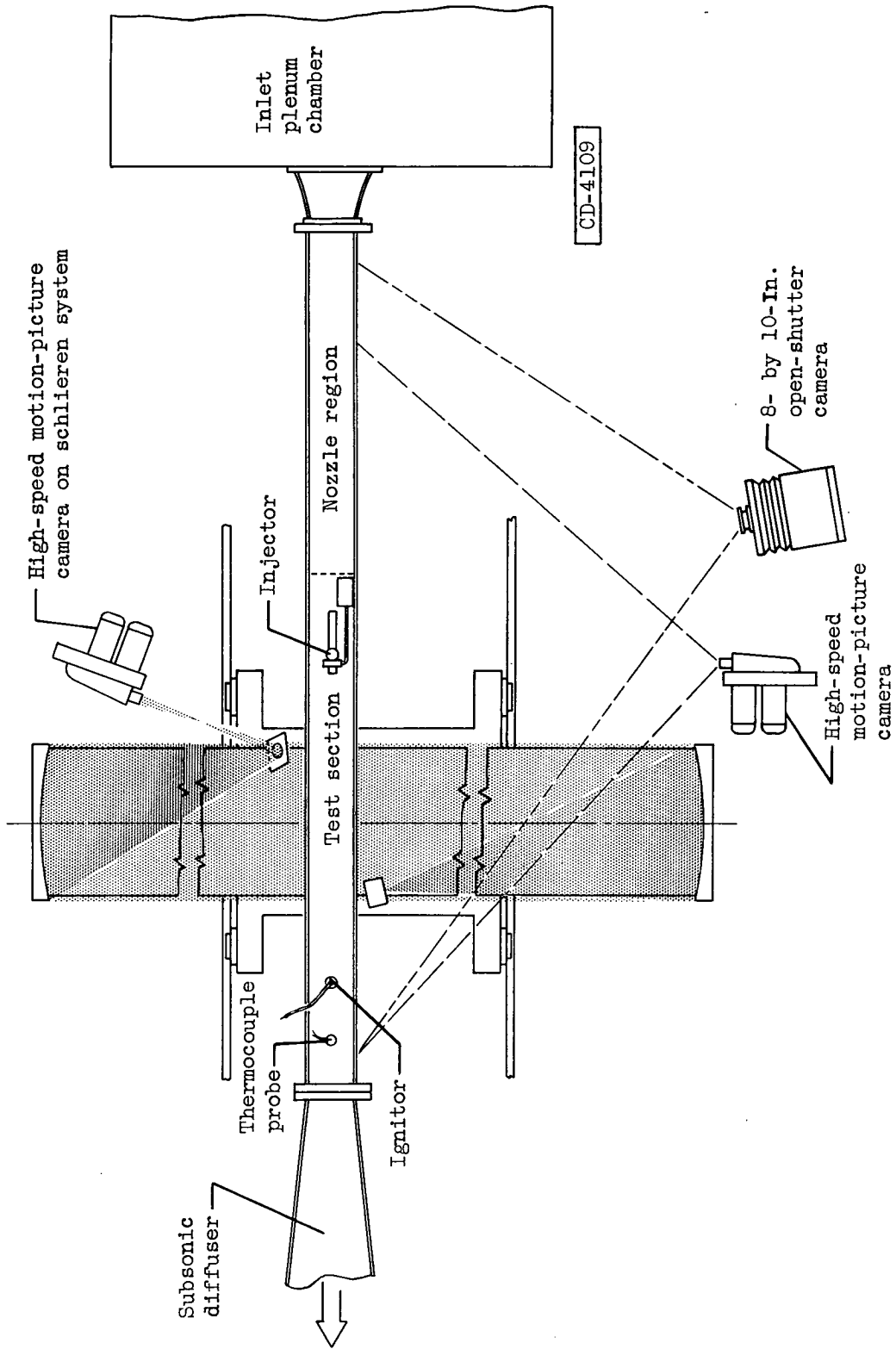
Run	Mach number	Volume of aluminum borohydride, cc	Ignition source	Injection pressure, lb/sq in. gage	Orifice diameter, in.	Duration of actual burning, sec	Observations	
1	1.5	5	None	10	1/32	1.0	Good steady burning	
5 6	2	5	None	7.5	1/32	---	} No ignition	
				3/64	---			
^a 11			Capsule	38	1/64	1.70	Burned very steadily over short distance after ignition	
12						.34	Burned as run 11, but orifice plugged during burning	
^b 13					28	1/32	0.44	Ignited with moderately loud bang and continued to burn steadily
^c 7		7	None	28	3/64	0.2	} After some delay, ignited and burned with pale blue-green flame	
8					---			
9 and 10		10	None	28	3/64	---		
2	3	10	None	7.5	1/32	---	} No ignition	
3		5	None	10	1/32	---		
4				30	1/32	---		
14		Capsule	28	$\sqrt{2}/64$	---			
15			38	$\sqrt{2}/64$	---			
16		Spark			28	$\sqrt{2}/64$	0.9	} Burned steadily after smooth ignition
17					1/64	1.8		
^d 18					38	1/64	1.9	

^aIllustrated in figure 12.

^bIllustrated in figure 14.

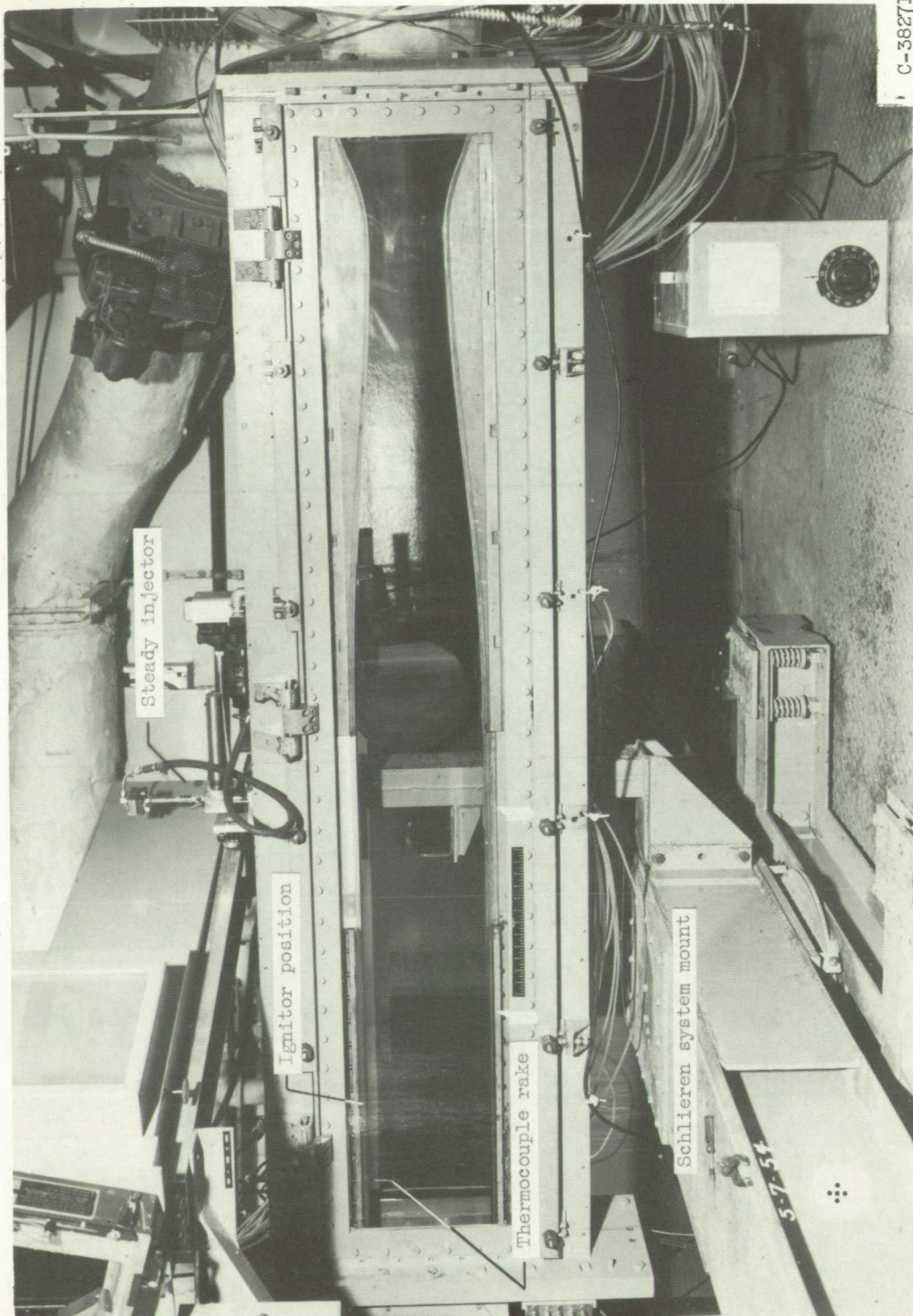
^cIllustrated in figure 11.

^dIllustrated in figure 13.



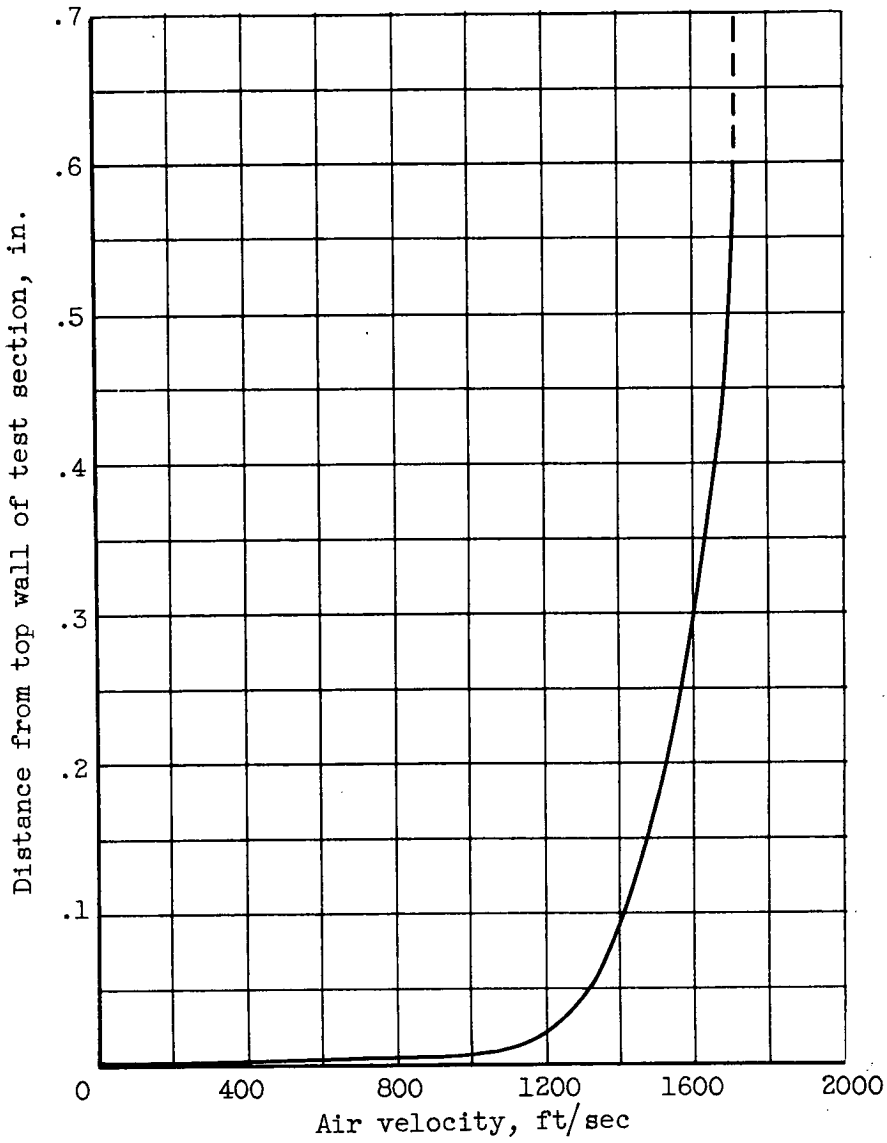
(a) Diagrammatic sketch viewed from top of tunnel, showing approximate camera positions.

Figure 1. - 3.84- by 10-Inch supersonic tunnel.



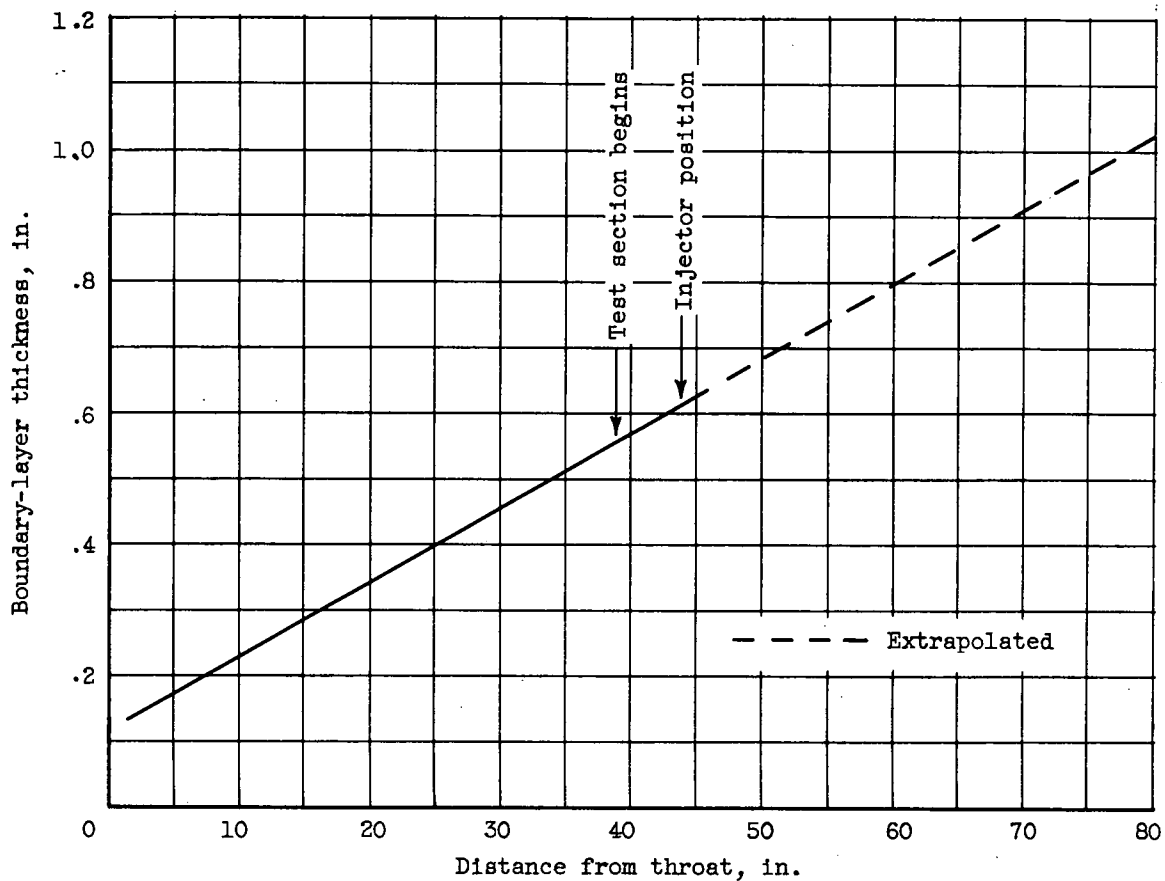
(b) Photograph showing steady-state injector and auxiliary equipment mounted on top wall of tunnel. Mach 2 nozzle blocks in place.

Figure 1. - Concluded. 3.84- by 10-Inch supersonic tunnel.



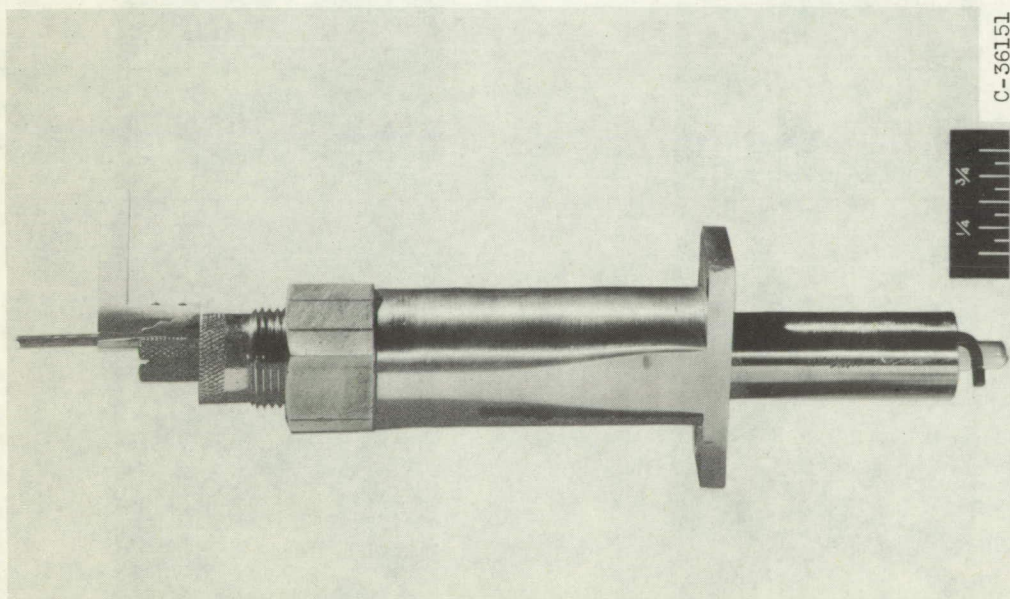
(a) Velocity profile through boundary layer at point of fuel injection (ref. 10).

Figure 2. - Boundary-layer flow in 3.84- by 10-inch supersonic wind tunnel at Mach 2.



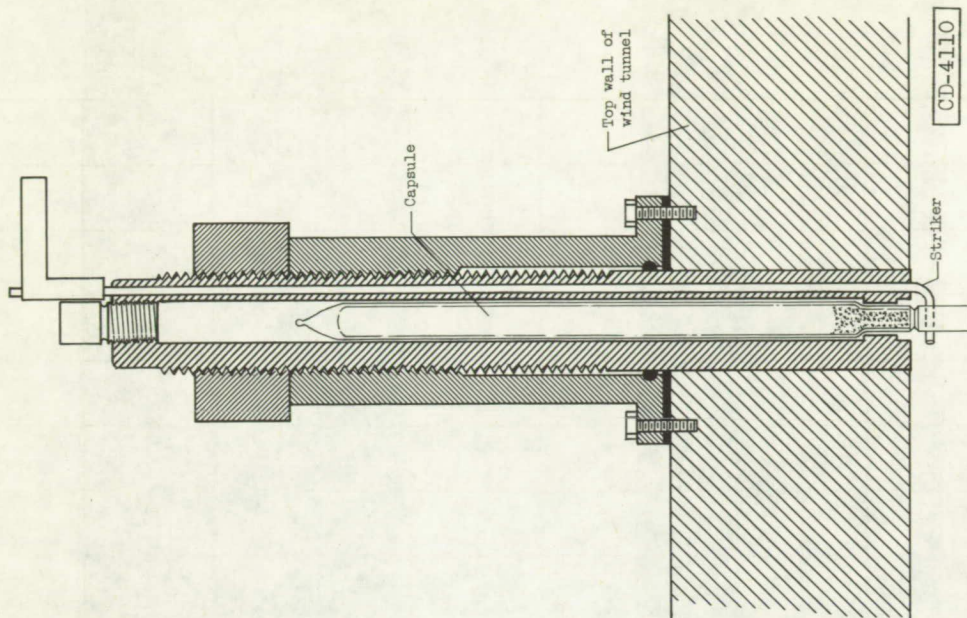
(b) Boundary-layer thickness as function of downstream distance from throat.

Figure 2. - Concluded. Boundary-layer flow in 3.84- by 10-inch supersonic wind tunnel at Mach 2.



C-36151

(a) Capsule-breaking device.



(b) Diagrammatic sketch of capsule-breaking device mounted in top wall of tunnel.

Figure 3. - Fuel injector for transient runs.

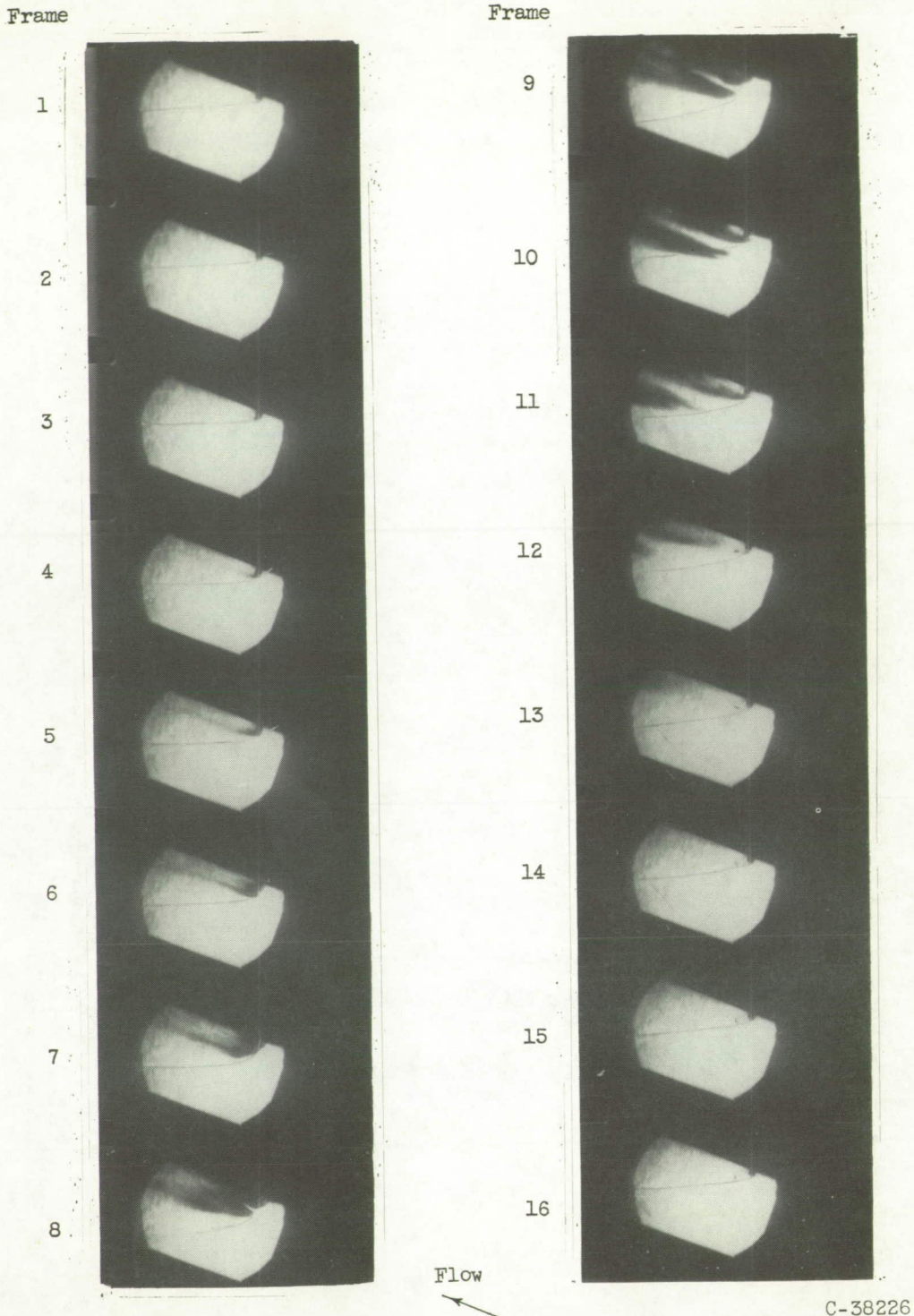


Figure 4. - High-speed schlieren motion pictures showing injection pattern of 1/2-cc liquid aluminum borohydride at Mach 4 (run 16, table III). (Aluminum borohydride shows up as a dark area, since combustion has not started. The shock wave has been retouched.)

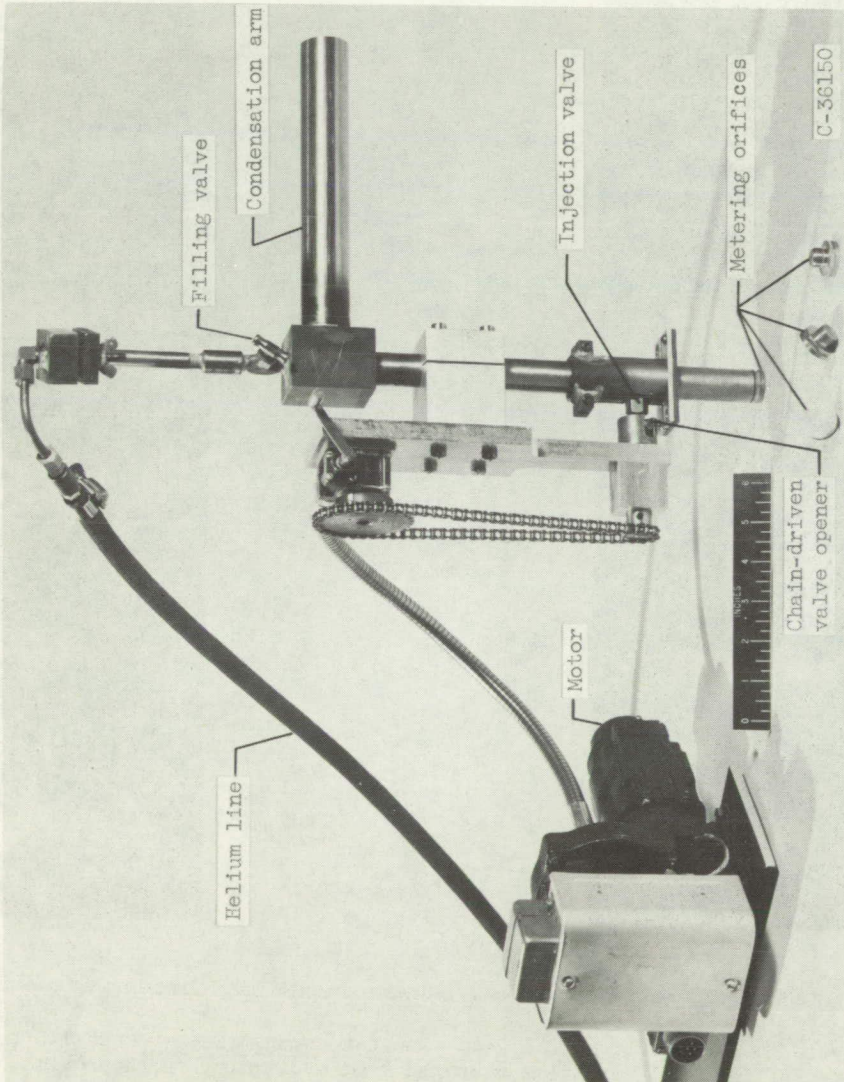
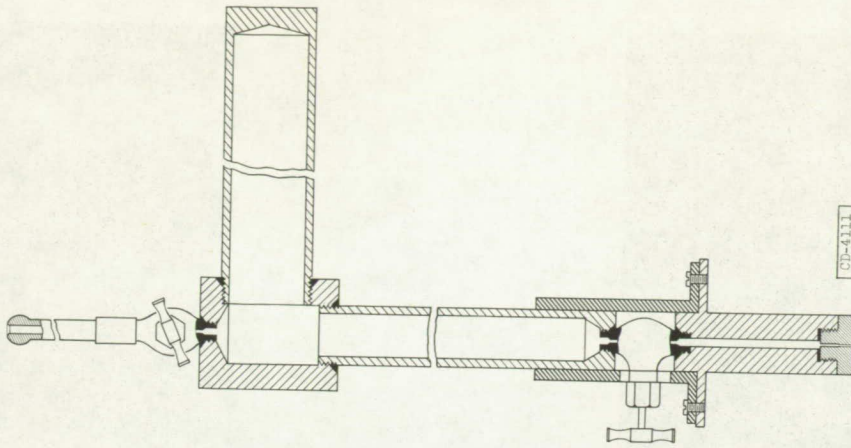
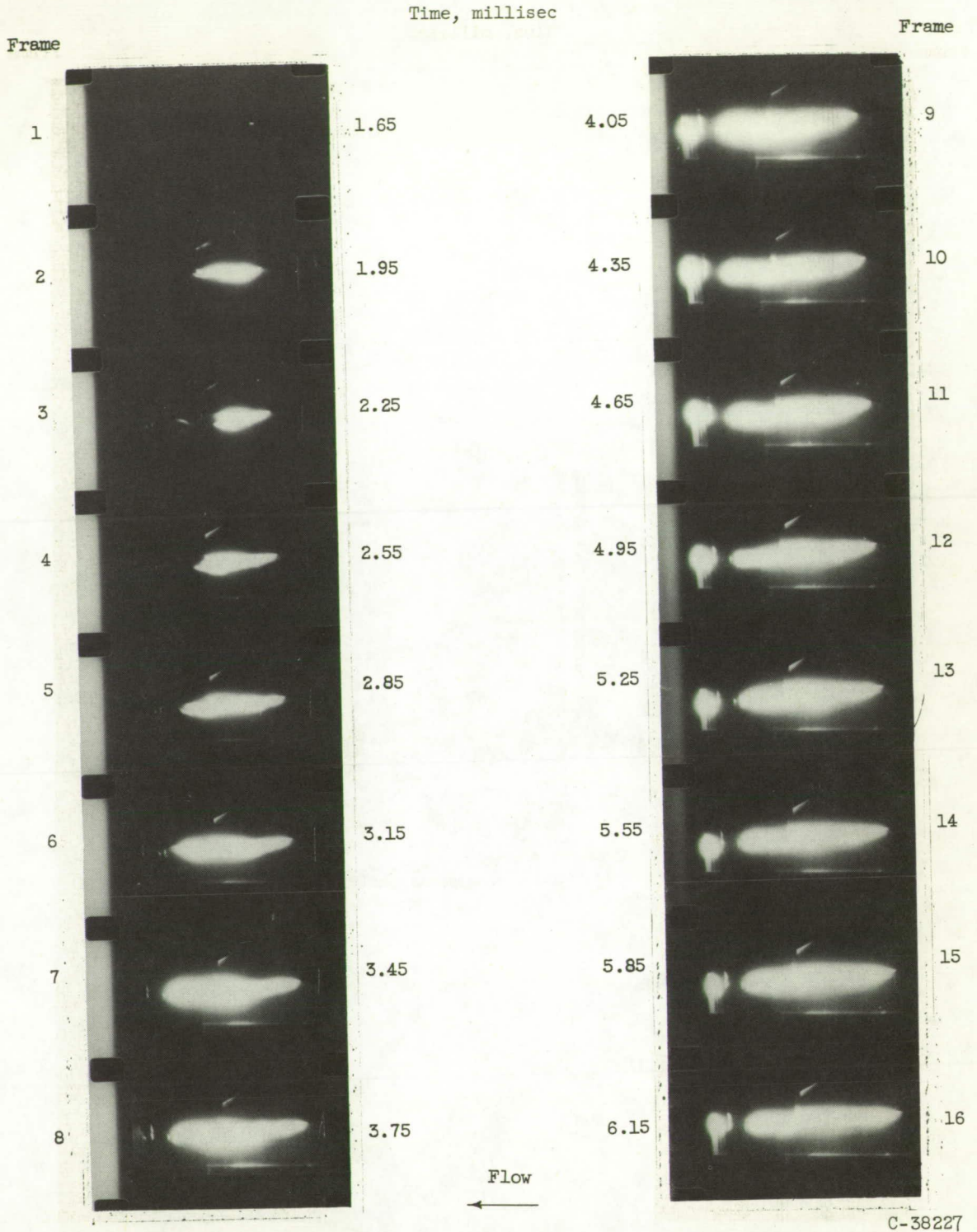
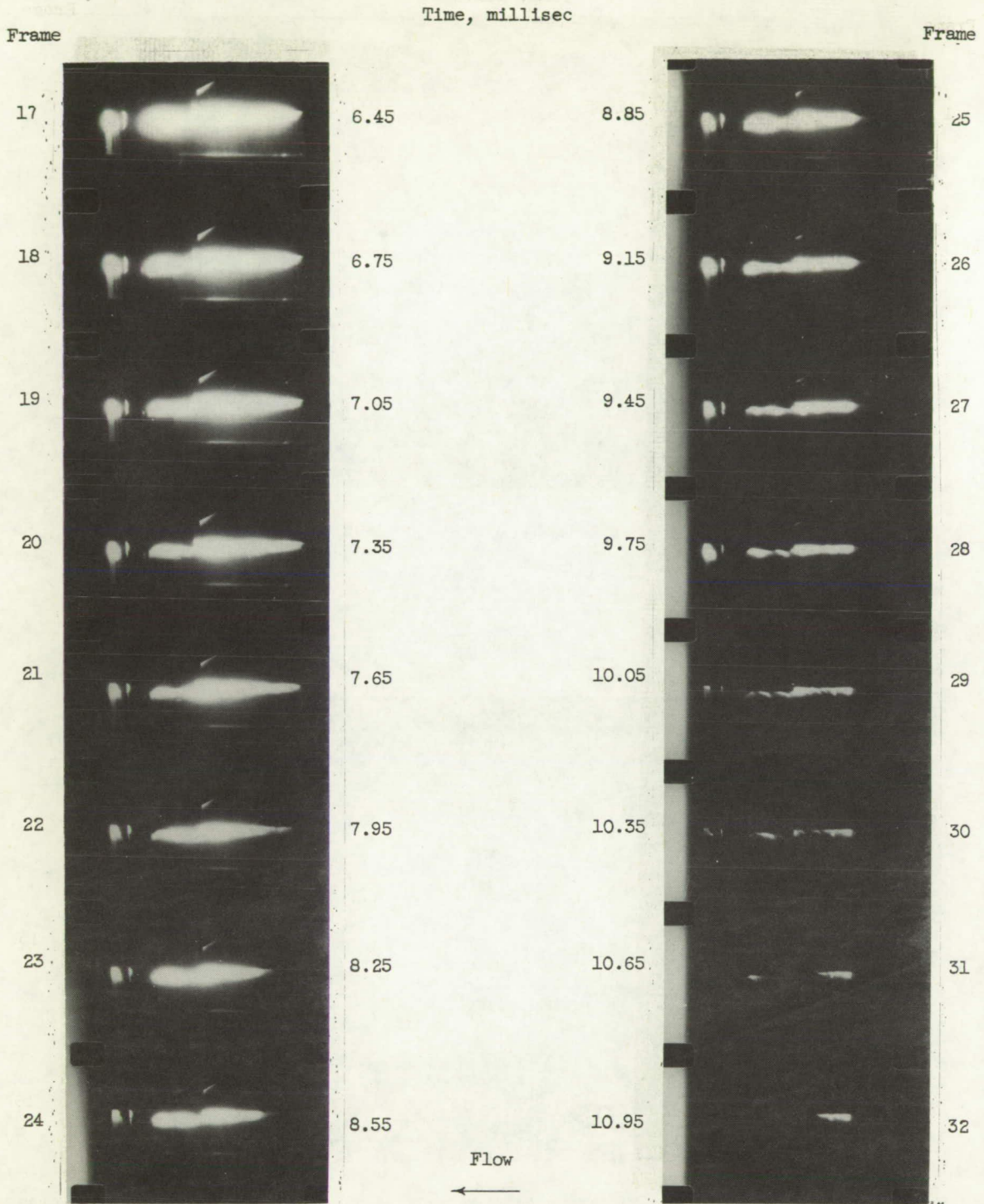


Figure 5. - Steady-state injector, showing auxiliary remote-control opening equipment and helium line.



(a) Direct motion pictures. Camera speed, 3333 frames per second.

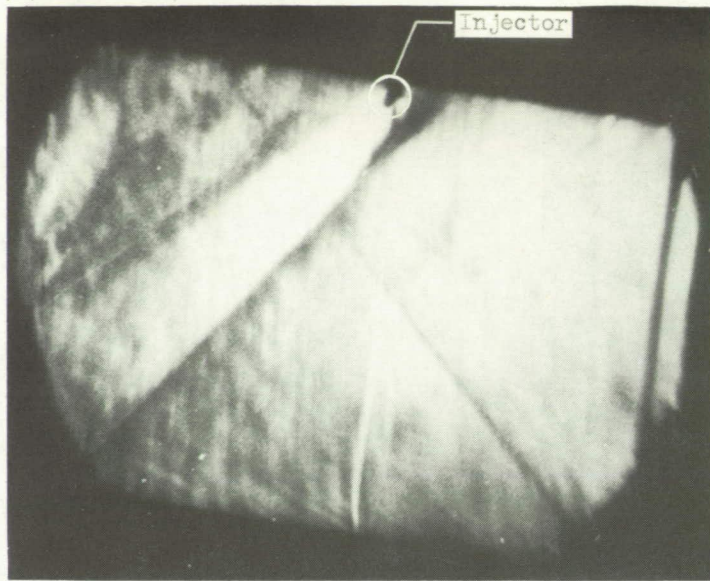
Figure 6. - Combustion of 1/2-cc aluminum borohydride at Mach 1.5 (run 37, table III). Elapsed time measured from arbitrary zero approximately 1.6 milliseconds before burning starts.



C-38228

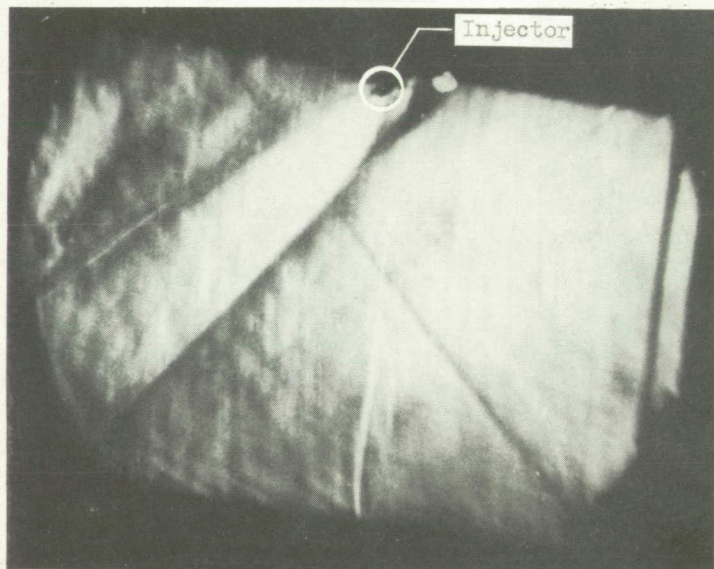
(a) Concluded. Direct motion pictures. Camera speed, 3333 frames per second.

Figure 6. - Continued. Combustion of 1/2-cc aluminum borohydride at Mach 1.5 (run 37, table III). Elapsed time measured from arbitrary zero approximately 1.6 milliseconds before burning starts.



Frame 1; 0.75 millisecc

Flow



Frame 2; 1.05 millisecc

C-38229

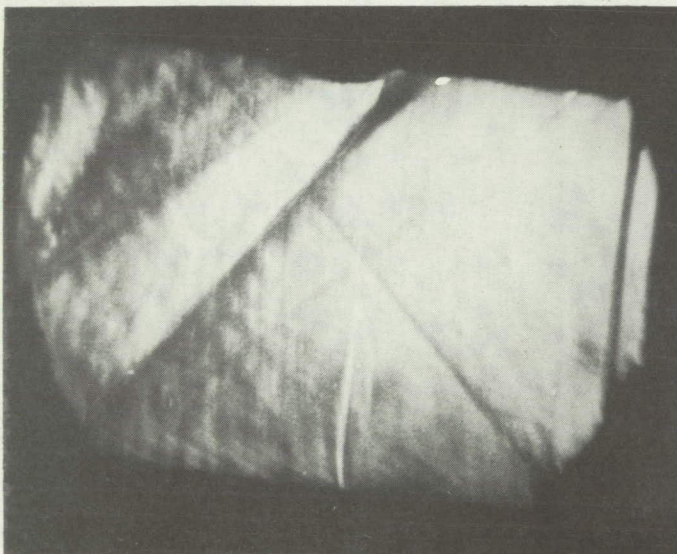
(b) Schlieren photographs of tunnel at injection point. Camera speed, 3348 frames per second.

Figure 6. - Continued. Combustion of 1/2-cc aluminum borohydride at Mach 1.5 (run 37, table III). Elapsed time measured from arbitrary zero approximately 1.6 milliseconds before burning starts.



Frame 3; 1.34 millise

Flow
←



Frame 4; 1.64 millise

C-38230

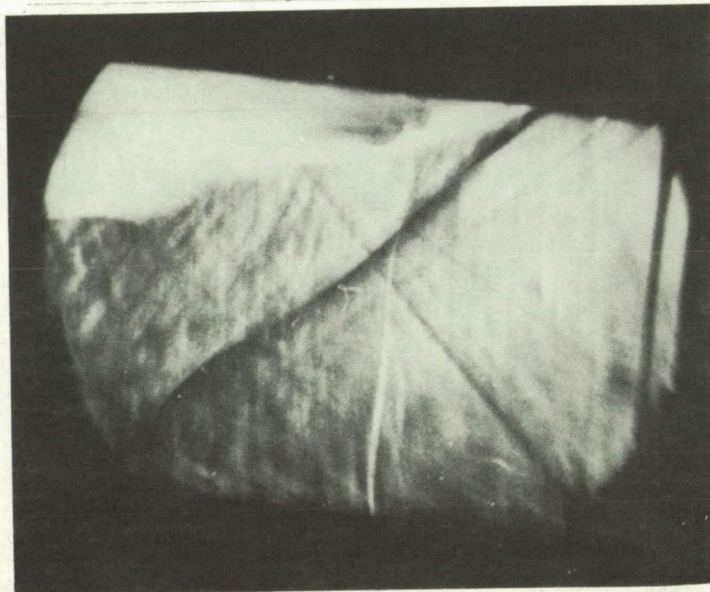
(b) Continued. Schlieren photographs of tunnel at injection point. Camera speed, 3348 frames per second.

Figure 6. - Continued. Combustion of 1/2-cc aluminum borohydride at Mach 1.5 (run 37, table III). Elapsed time measured from arbitrary zero approximately 1.6 milliseconds before burning starts.



Frame 5; 1.94 millisec

Flow



Frame 6; 2.24 millisec

C-38231

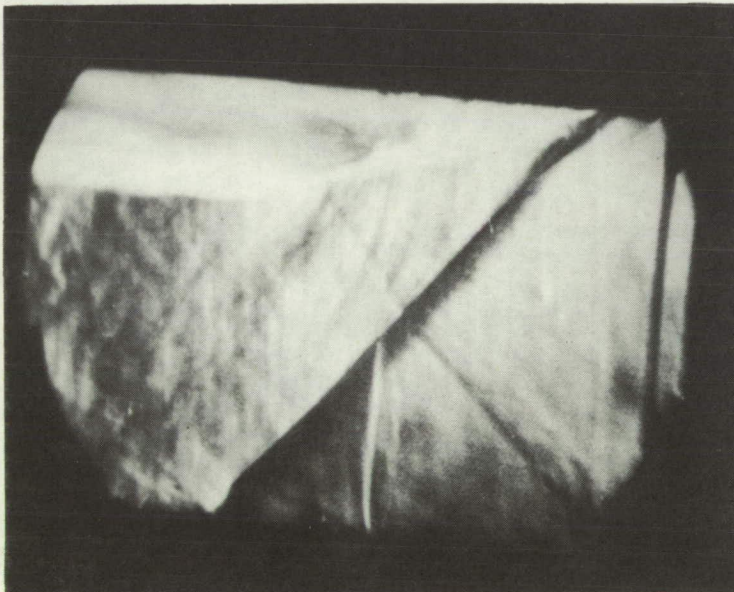
(b) Continued. Schlieren photographs of tunnel at injection point. Camera speed, 3348 frames per second.

Figure 6. - Continued. Combustion of 1/2-cc aluminum borohydride at Mach 1.5 (run 37, table III). Elapsed time measured from arbitrary zero approximately 1.6 milliseconds before burning starts.



Frame 7; 2.54 millisecc

Flow

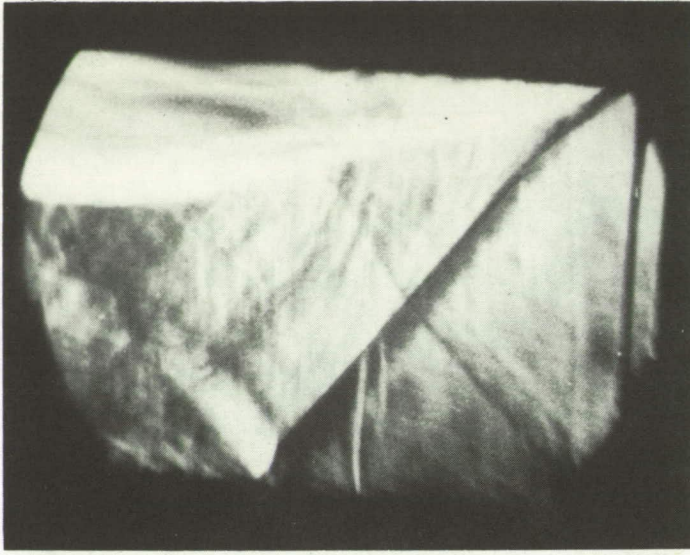


Frame 8; 2.84 millisecc

C-38232

(b) Continued. Schlieren photographs of tunnel at injection point. Camera speed, 3348 frames per second.

Figure 6. - Continued. Combustion of 1/2-cc aluminum borohydride at Mach 1.5 (run 37, table III). Elapsed time measured from arbitrary zero approximately 1.6 milliseconds before burning starts.



Frame 9; 3.14 millisecc

Flow



Frame 10; 3.44 millisecc

! C-38233

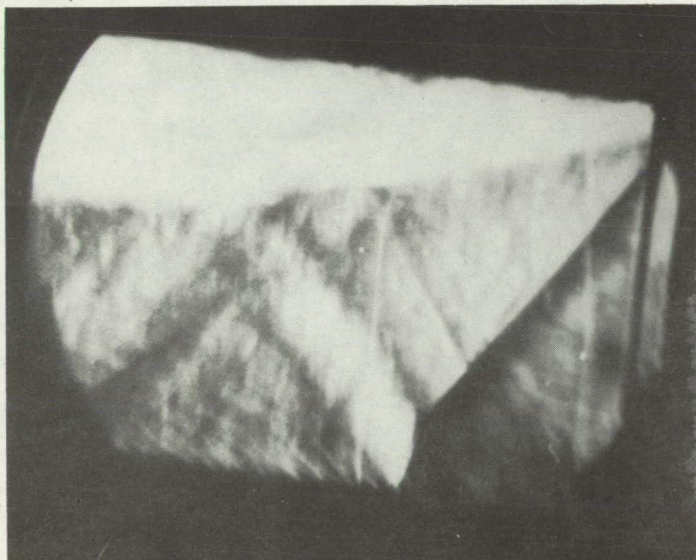
(b) Continued. Schlieren photographs of tunnel at injection point. Camera speed, 3348 frames per second.

Figure 6. - Continued. Combustion of 1/2-cc aluminum borohydride at Mach 1.5 (run 37, table III). Elapsed time measured from arbitrary zero approximately 1.6 milliseconds before burning starts.



Frame 11; 3.73 millisecc

Flow
←



Frame 12; 4.03 millisecc

C-38234

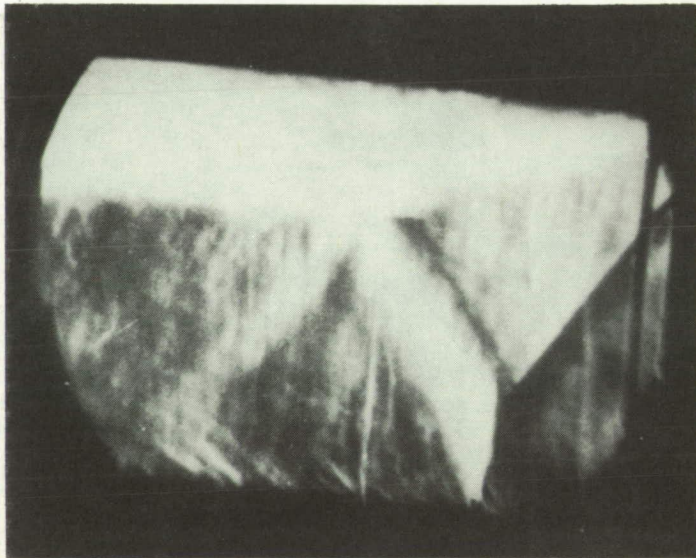
(b) Continued. Schlieren photographs of tunnel at injection point. Camera speed, 3348 frames per second.

Figure 6. - Continued. Combustion of 1/2-cc aluminum borohydride at Mach 1.5 (run 37, table III). Elapsed time measured from arbitrary zero approximately 1.6 milliseconds before burning starts.



Frame 13; 4.33 millisecc

Flow

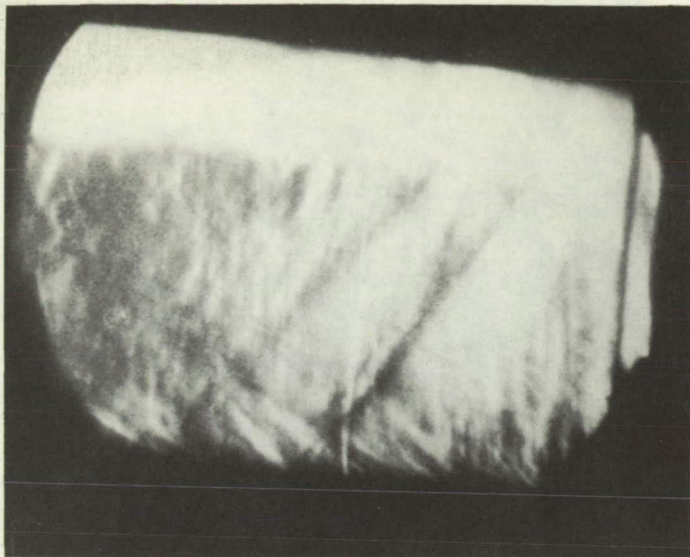


Frame 14; 4.63 millisecc

C-38235

(b) Continued. Schlieren photographs of tunnel at injection point. Camera speed, 3348 frames per second.

Figure 6. - Continued. Combustion of 1/2-cc aluminum borohydride at Mach 1.5 (run 37, table III). Elapsed time measured from arbitrary zero approximately 1.6 milliseconds before burning starts.



Frame 19; 6.12 millisec

Flow

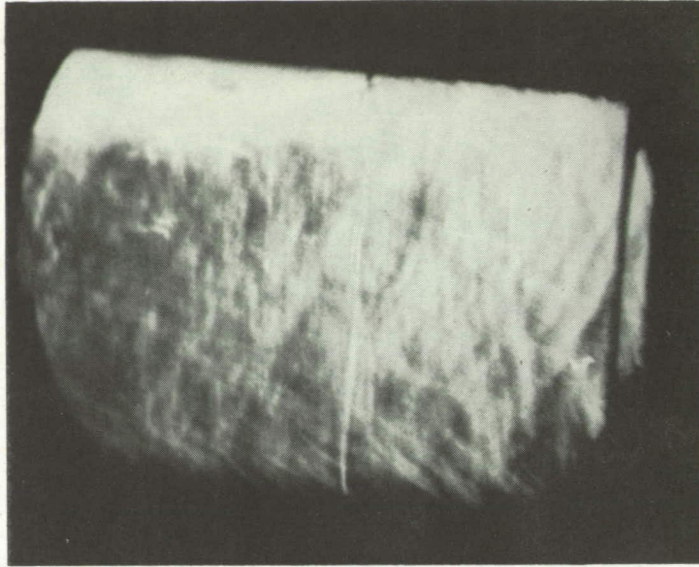


Frame 22; 7.02 millisec

C-38236

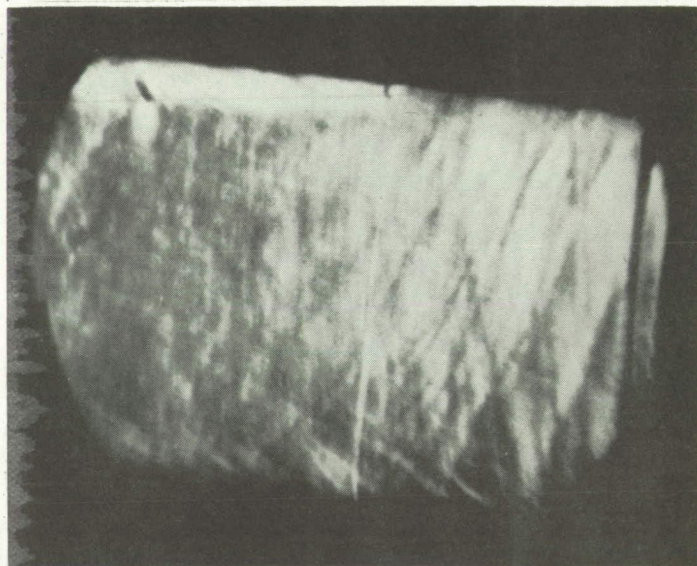
(b) Continued. Schlieren photographs of tunnel at injection point. Camera speed, 3348 frames per second.

Figure 6. - Continued. Combustion of 1/2-cc aluminum borohydride at Mach 1.5 (run 37, table III). Elapsed time measured from arbitrary zero approximately 1.6 milliseconds before burning starts.



Frame 27; 8.51 millisecc

Flow

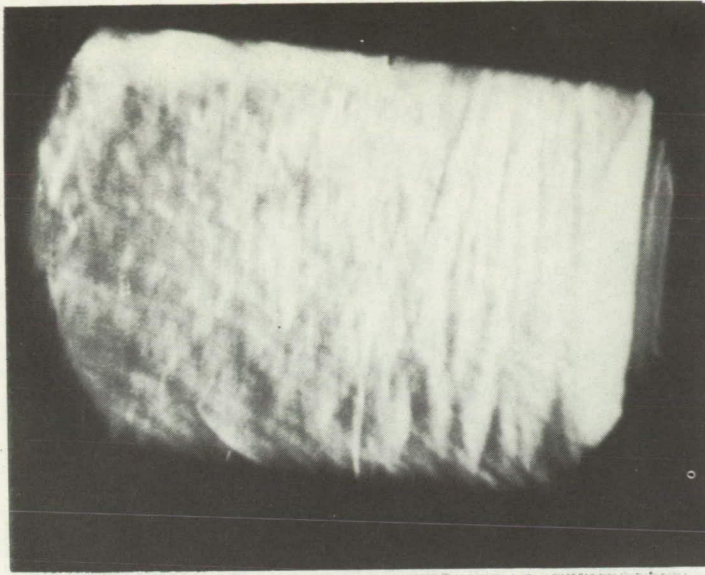


Frame 40; 12.40 millisecc

C-38237

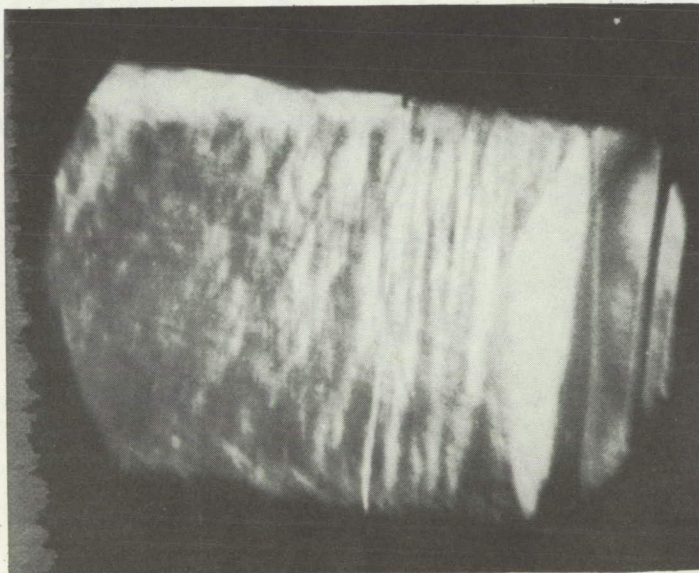
(b) Continued. Schlieren photographs of tunnel at injection point. Camera speed, 3348 frames per second.

Figure 6. - Continued. Combustion of 1/2-cc aluminum borohydride at Mach 1.5 (run 37, table III). Elapsed time measured from arbitrary zero approximately 1.6 milliseconds before burning starts.



Frame 58; 17.77 millisec

Flow

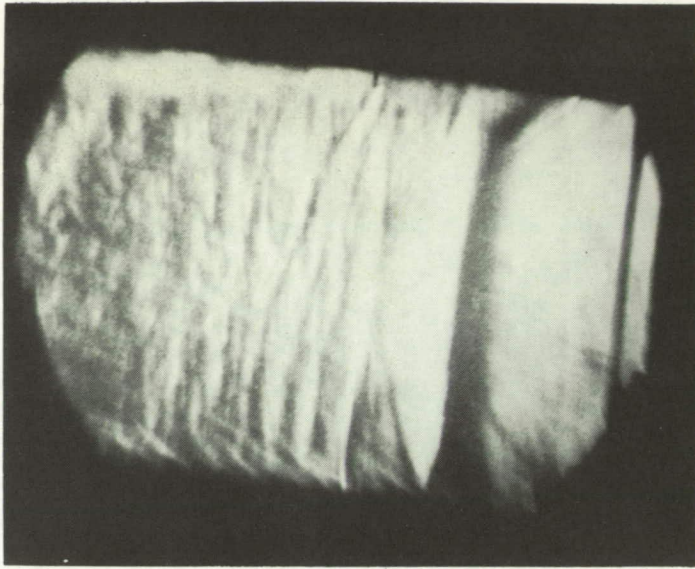


Frame 71; 21.66 millisec

C-38238

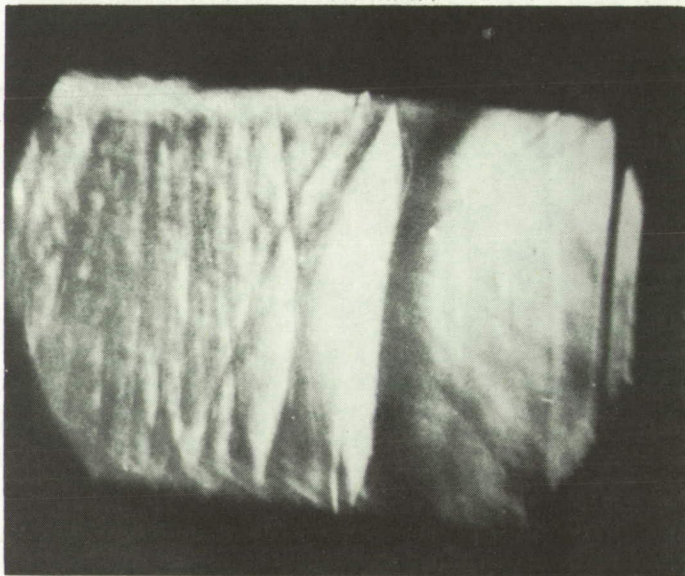
(b) Continued. Schlieren photographs of tunnel at injection point. Camera speed, 3348 frames per second.

Figure 6. - Continued. Combustion of 1/2-cc aluminum borohydride at Mach 1.5 (run 37, table III). Elapsed time measured from arbitrary zero approximately 1.6 milliseconds before burning starts.



Frame 83; 25.24 millisec

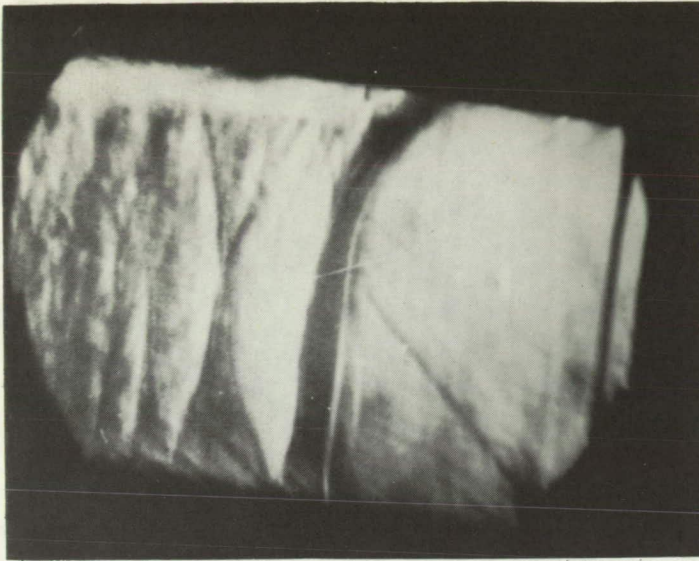
Flow



Frame 92; 27.93 millisec | C-38239

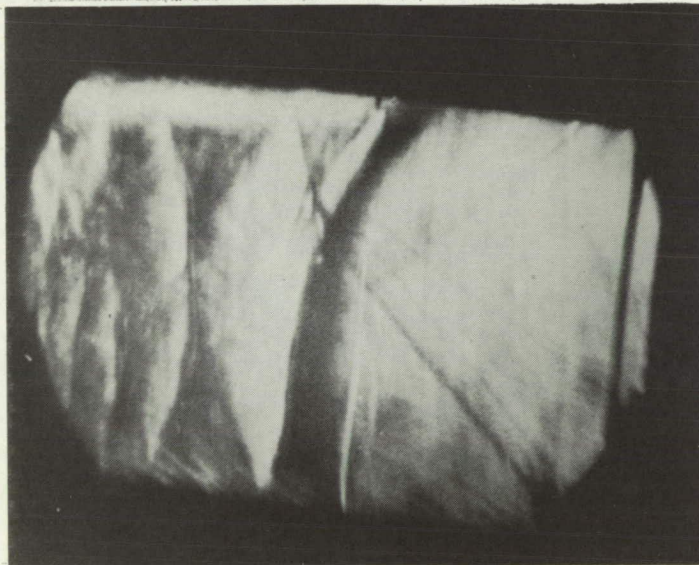
(b) Continued. Schlieren photographs of tunnel at injection point. Camera speed, 3348 frames per second.

Figure 6. - Continued. Combustion of 1/2-cc aluminum borohydride at Mach 1.5 (run 37, table III). Elapsed time measured from arbitrary zero approximately 1.6 milliseconds before burning starts.



Frame 104; 31.51 millisecc

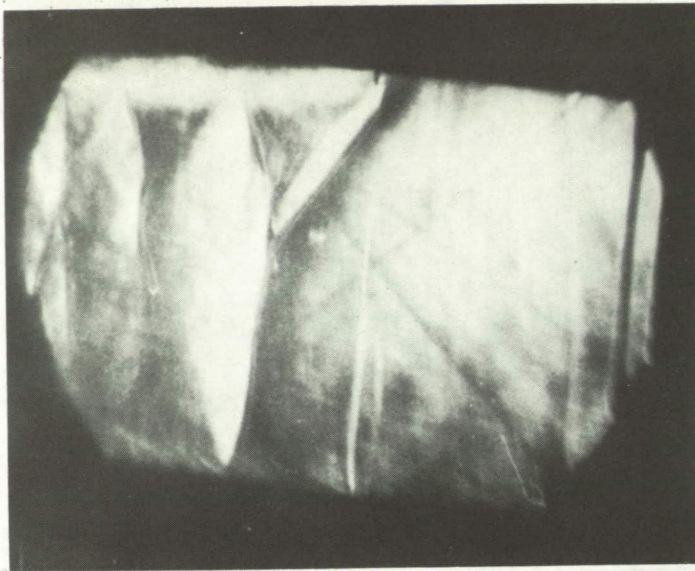
Flow



Frame 110; 33.30 millisecc C-38240

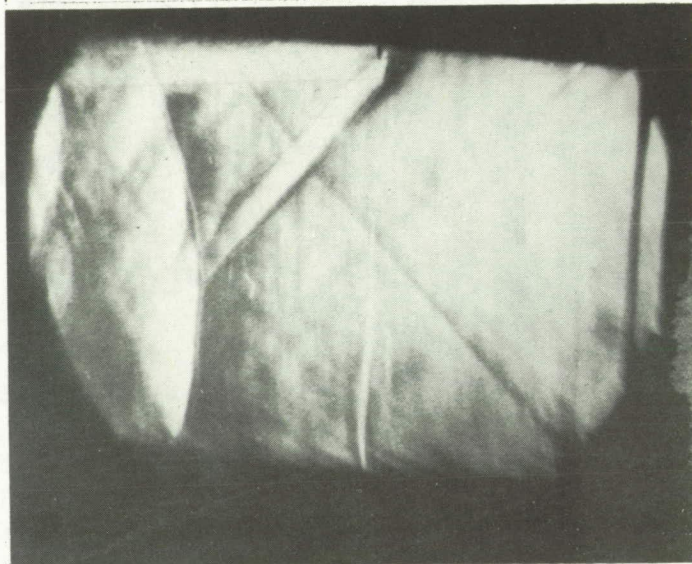
(b) Continued. Schlieren photographs of tunnel at injection point. Camera speed, 3348 frames per second.

Figure 6. - Continued. Combustion of 1/2-cc aluminum borohydride at Mach 1.5 (run 37, table III). Elapsed time measured from arbitrary zero approximately 1.6 milliseconds before burning starts.



Frame 119; 35.99 millisecc

Flow
←



Frame 133; 40.17 millisecc

C-38241

(b) Continued. Schlieren photographs of tunnel at injection point. Camera speed, 3348 frames per second.

Figure 6. - Continued. Combustion of 1/2-cc aluminum borohydride at Mach 1.5 (run 37, table III). Elapsed time measured from arbitrary zero approximately 1.6 milliseconds before burning starts.



Frame 150; 45.25 millisecc

Flow
←



Frame 165; 49.73 millisecc C-38242

(b) Continued. Schlieren photographs of tunnel at injection point. Camera speed, 3348 frames per second.

Figure 6. - Continued. Combustion of 1/2-cc aluminum borohydride at Mach 1.5 (run 37, table III). Elapsed time measured from arbitrary zero approximately 1.6 milliseconds before burning starts.

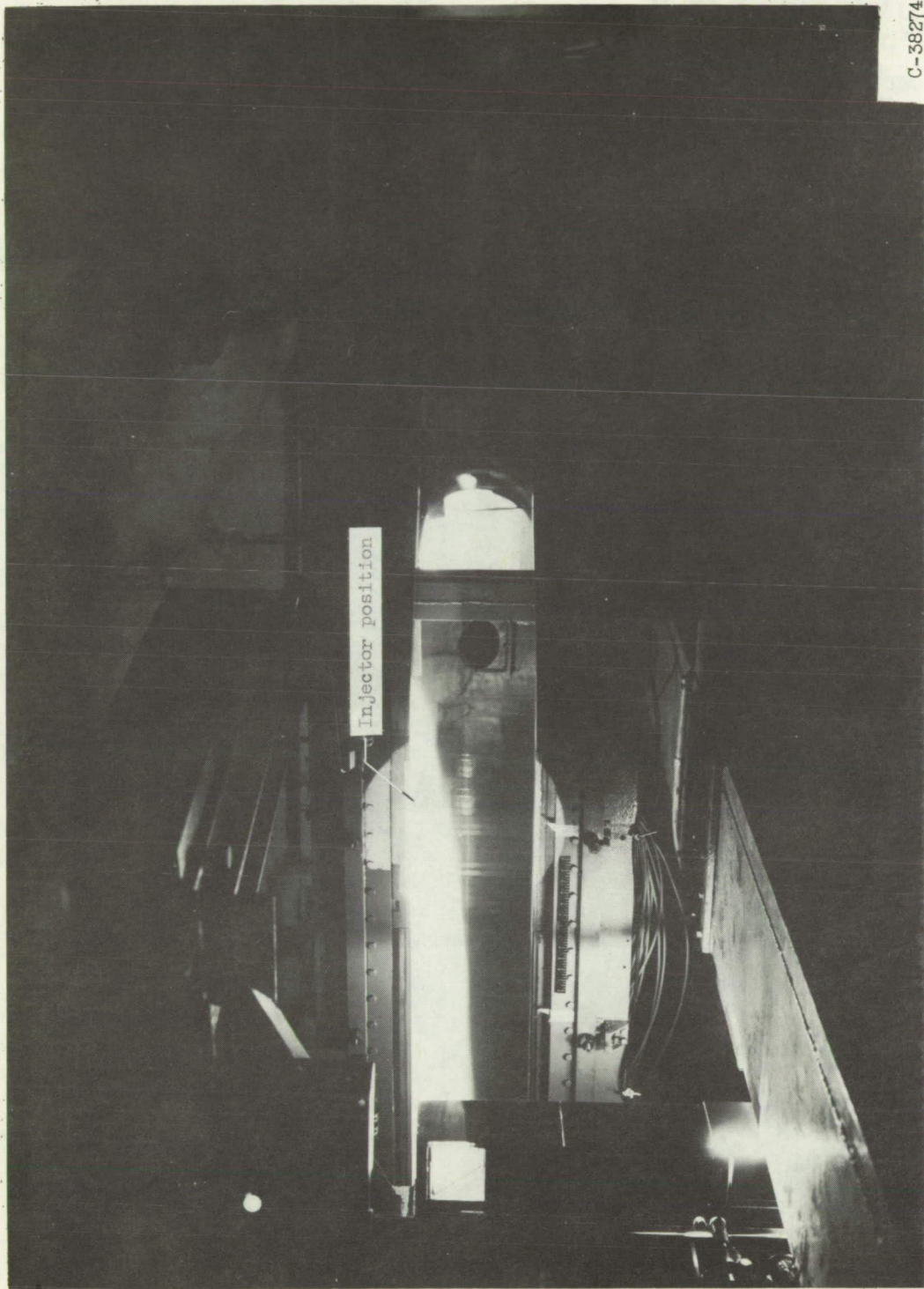


Frame 200; 60.19 millisecc

C-38269

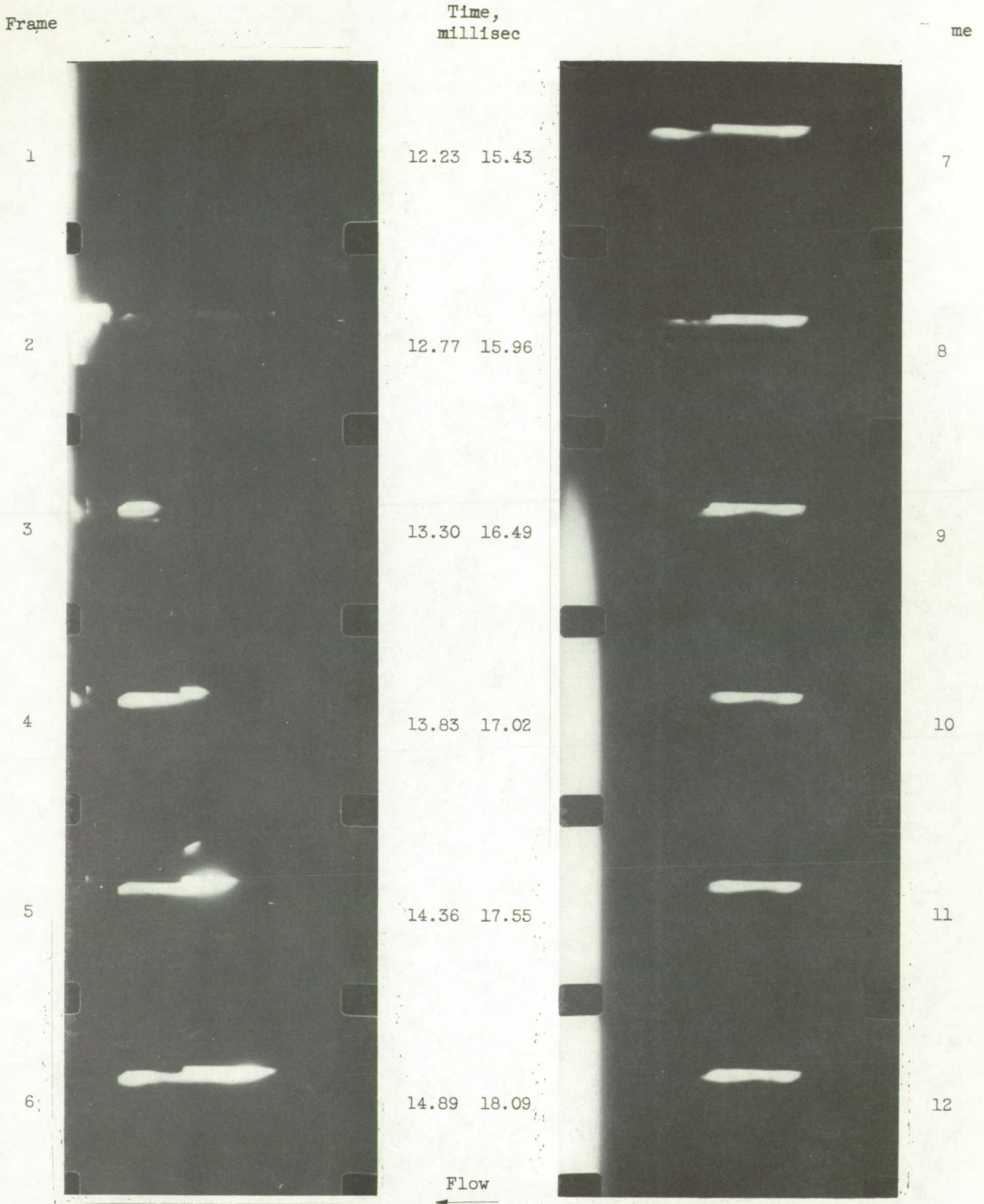
(b) Concluded. Schlieren photographs of tunnel at injection point.
Camera speed, 3348 frames per second.

Figure 6. - Concluded. Combustion of 1/2-cc aluminum borohydride at
Mach 1.5 (run 37, table III). Elapsed time measured from arbitrary
zero approximately 1.6 milliseconds before burning starts.



C-38274

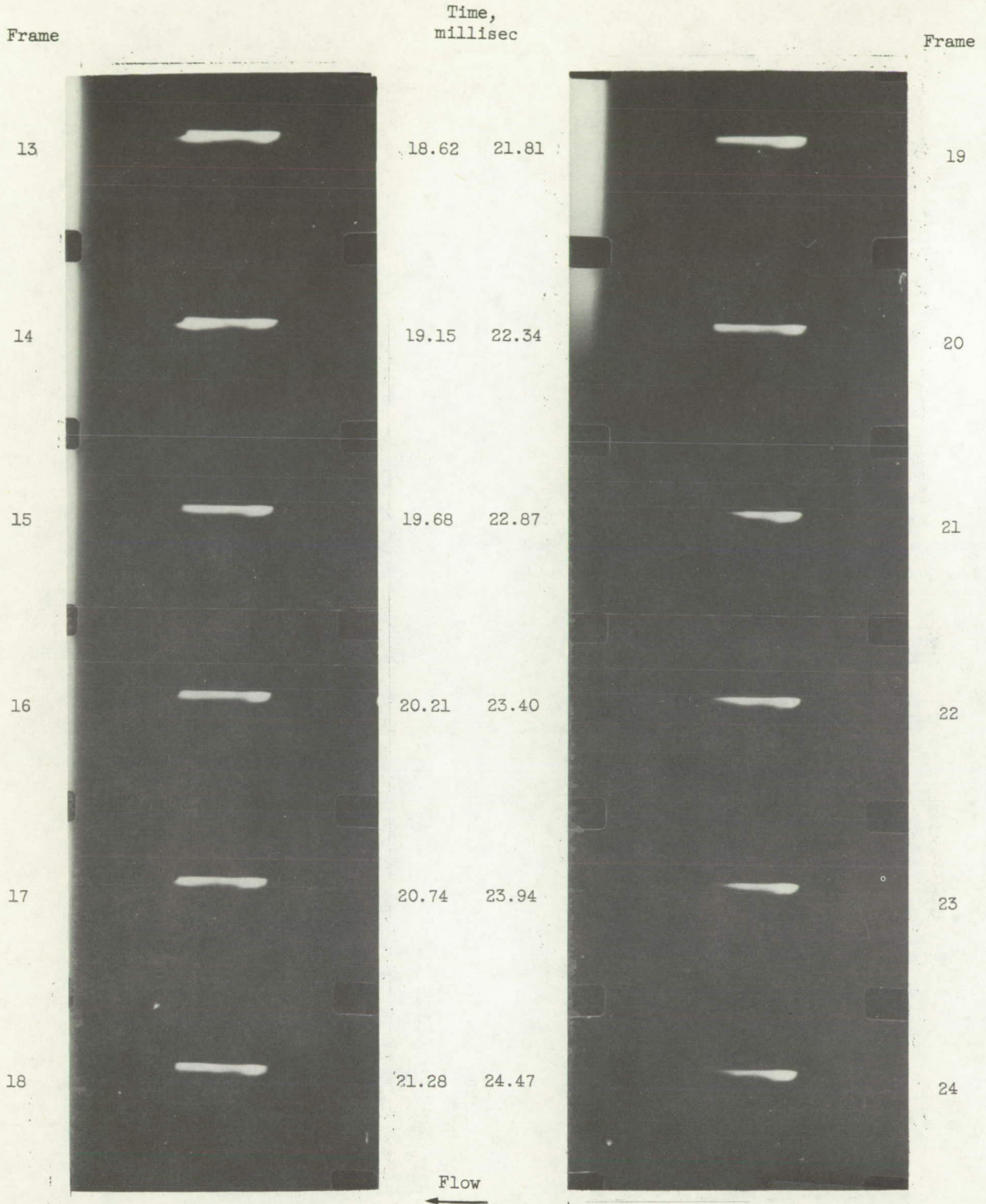
Figure 7. - Open-shutter photograph of transient combustion of 1/2-cc aluminum borohydride at Mach 1.5 (run 37, table III).



(a) Direct motion pictures. Camera speed, 1880 frames per second. Spontaneous ignition occurred in diffuser.

C-38243

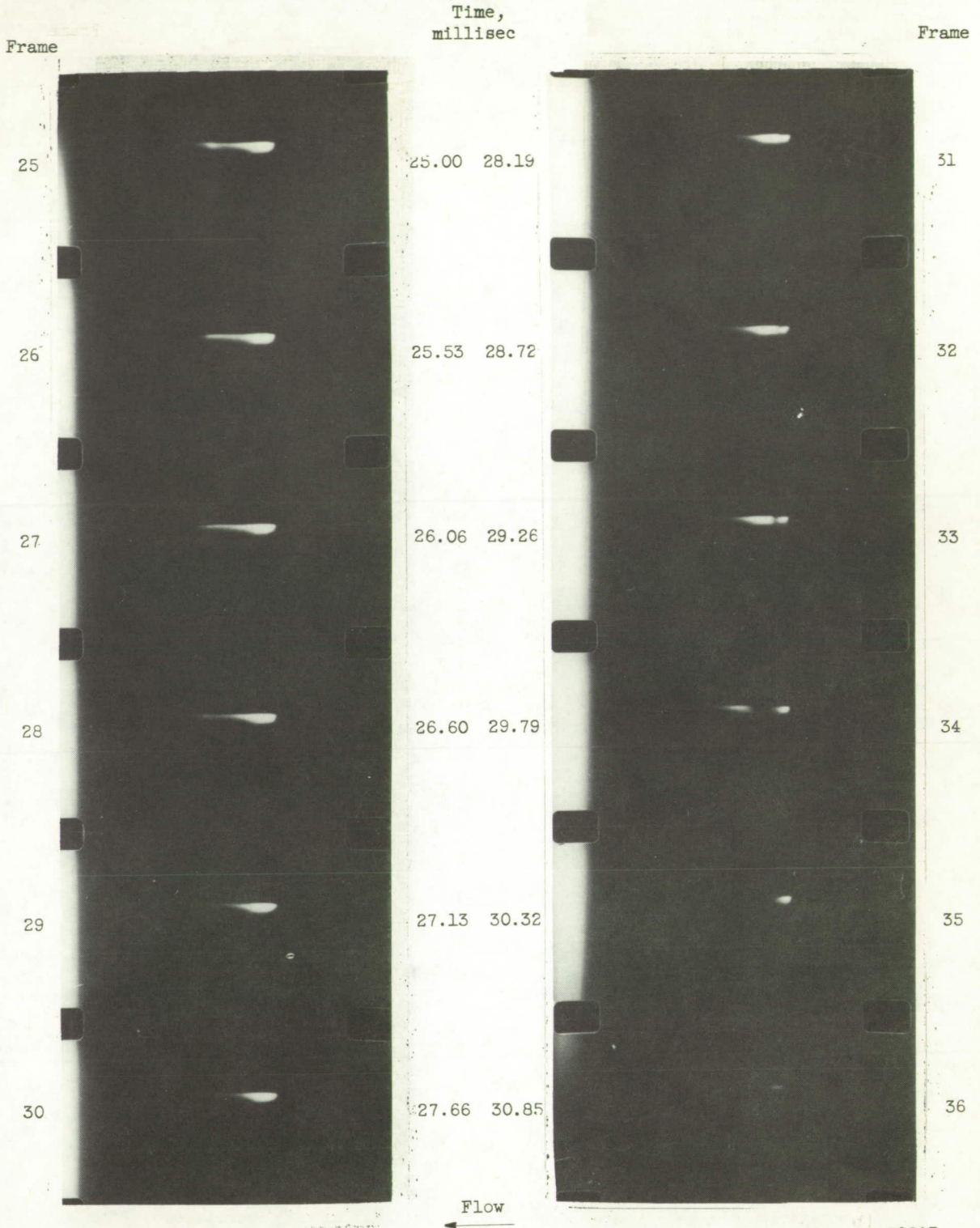
Figure 8. - Combustion of 1/2-cc aluminum borohydride at Mach 3 (run 25, table III).



C-38244

(a) Continued. Direct motion pictures. Camera speed, 1880 frames per second. Spontaneous ignition occurred in diffuser.

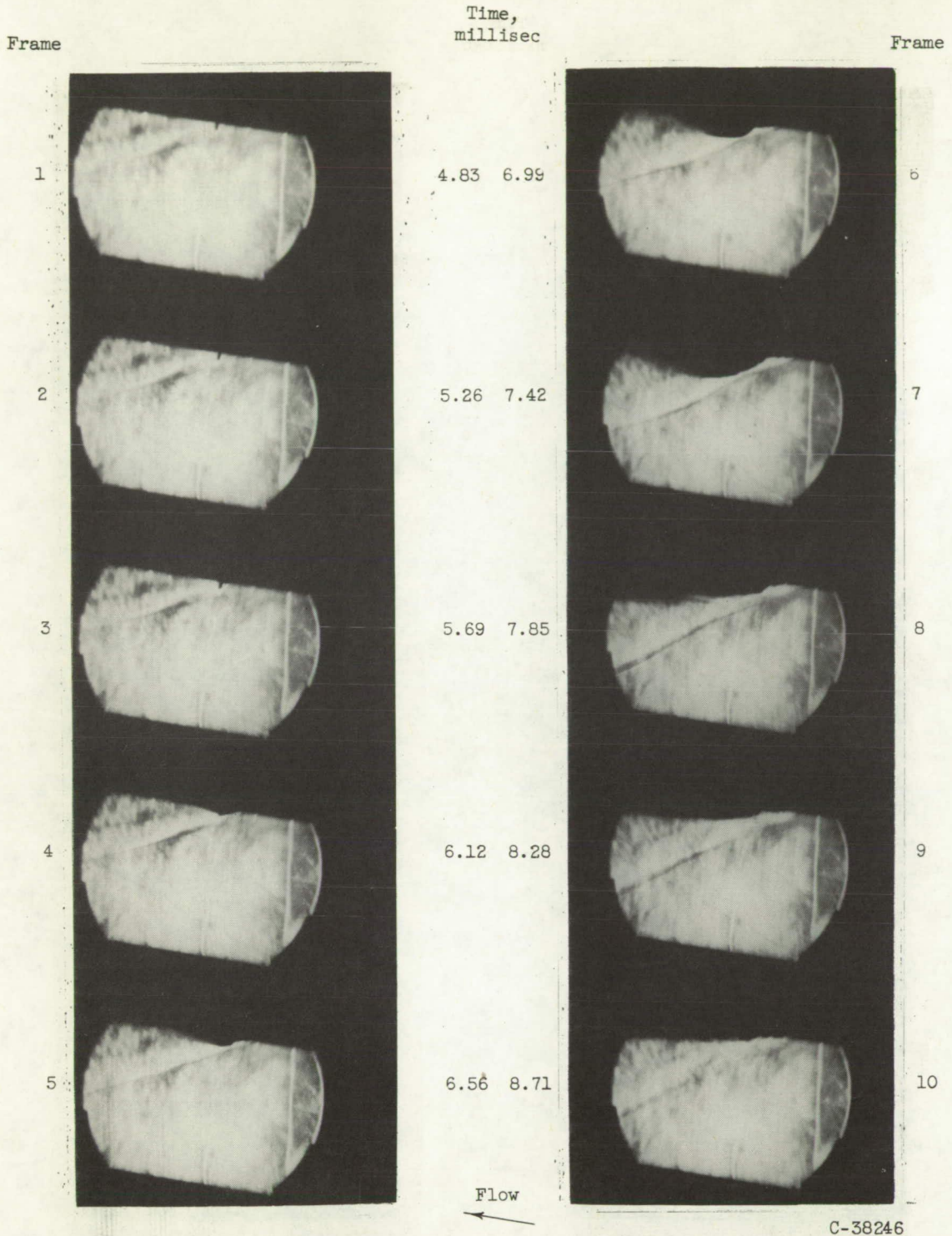
Figure 8. - Continued. Combustion of 1/2-cc aluminum borohydride at Mach 3 (run 25, table III).



C-38245

(a) Concluded. Direct motion pictures. Camera speed, 1880 frames per second. Spontaneous ignition occurred in diffuser.

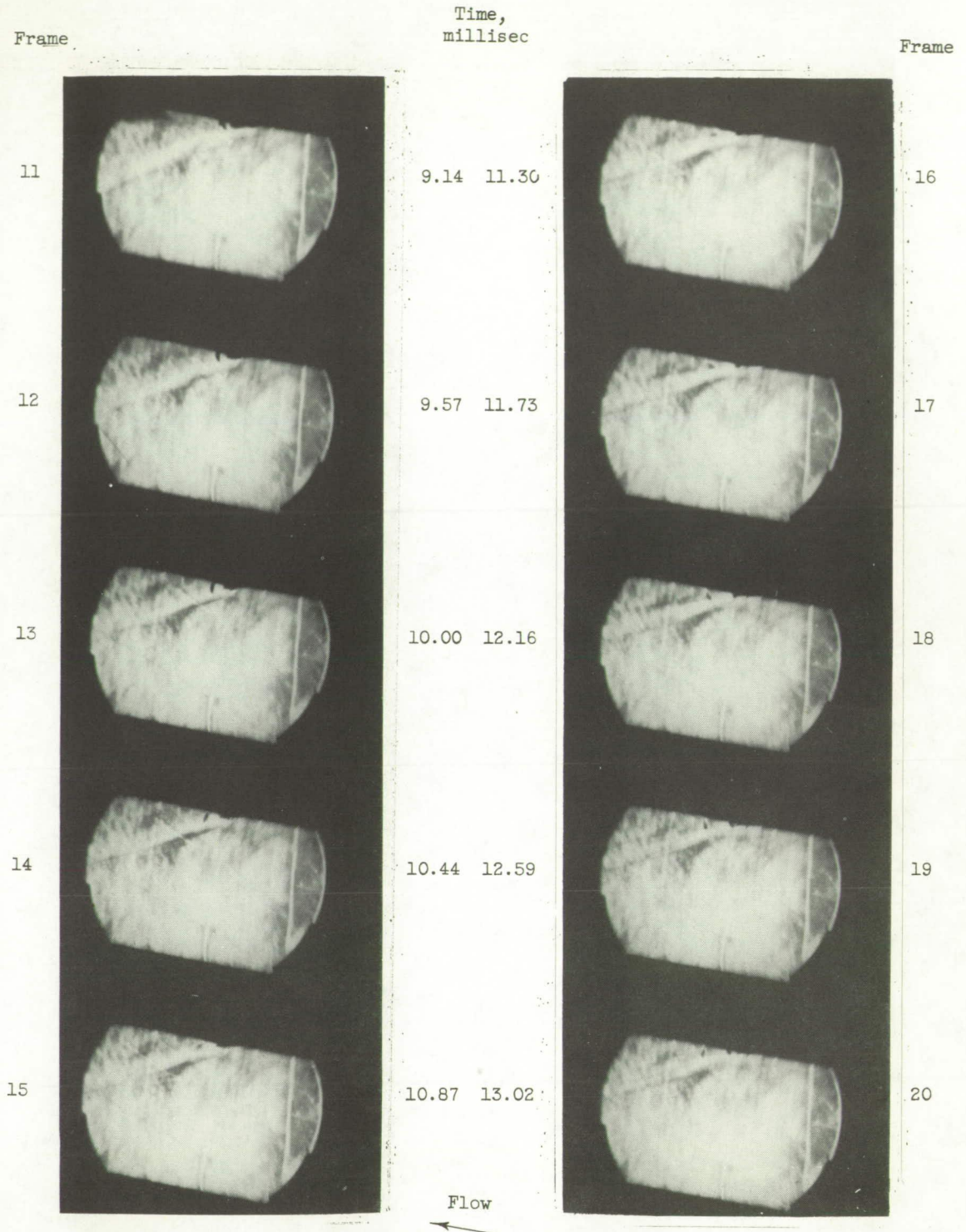
Figure 8. - Continued. Combustion of 1/2-cc aluminum borohydride at Mach 3 (run 25, table III).



C-38246

(b) Schlieren photographs of tunnel at injection point. Camera speed, 2319 frames per second.

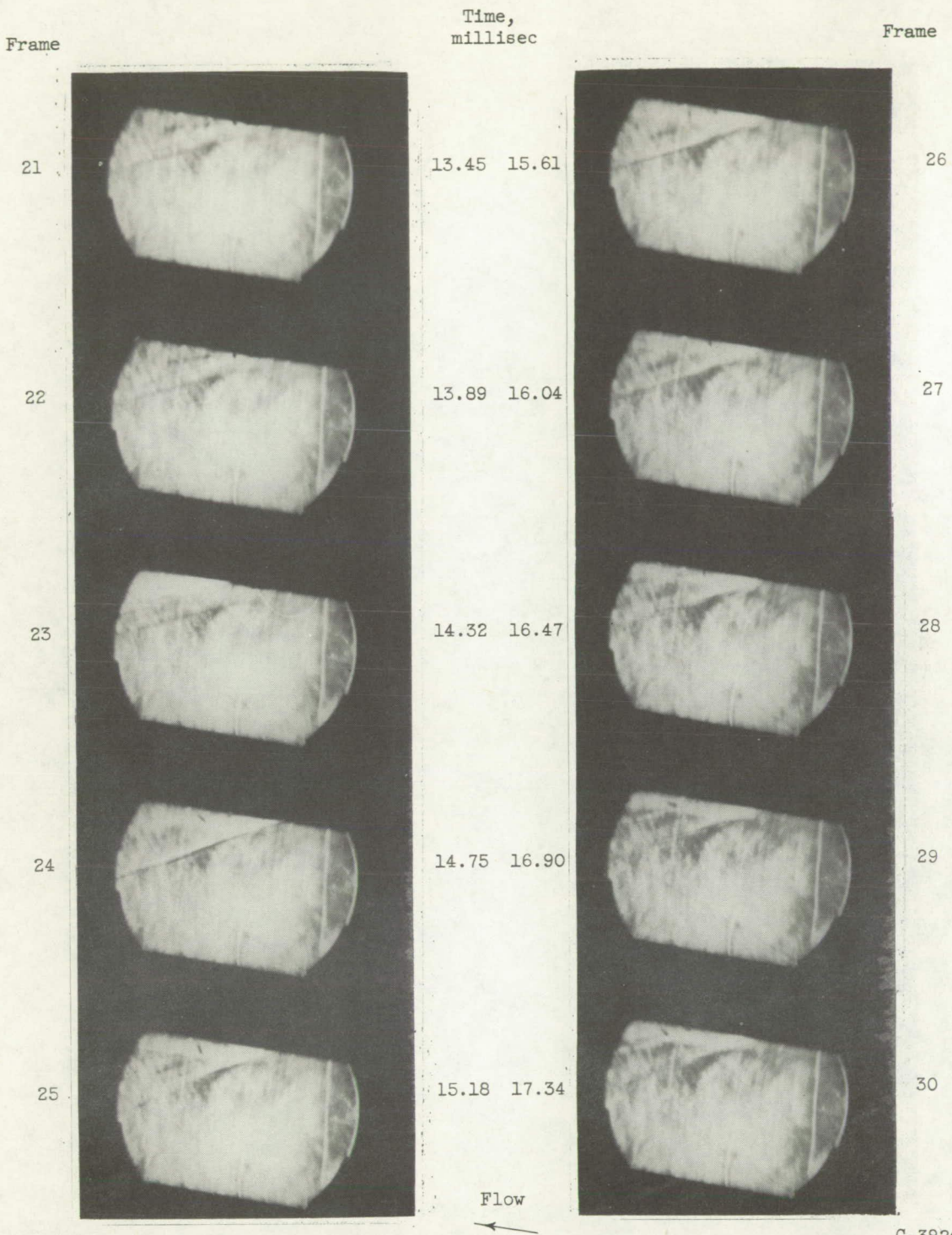
Figure 8. - Continued. Combustion of 1/2-cc aluminum borohydride at Mach 3 (run 25, table III).



C-38247

(b) Continued. Schlieren photographs of tunnel at injection point. Camera speed, 2319 frames per second.

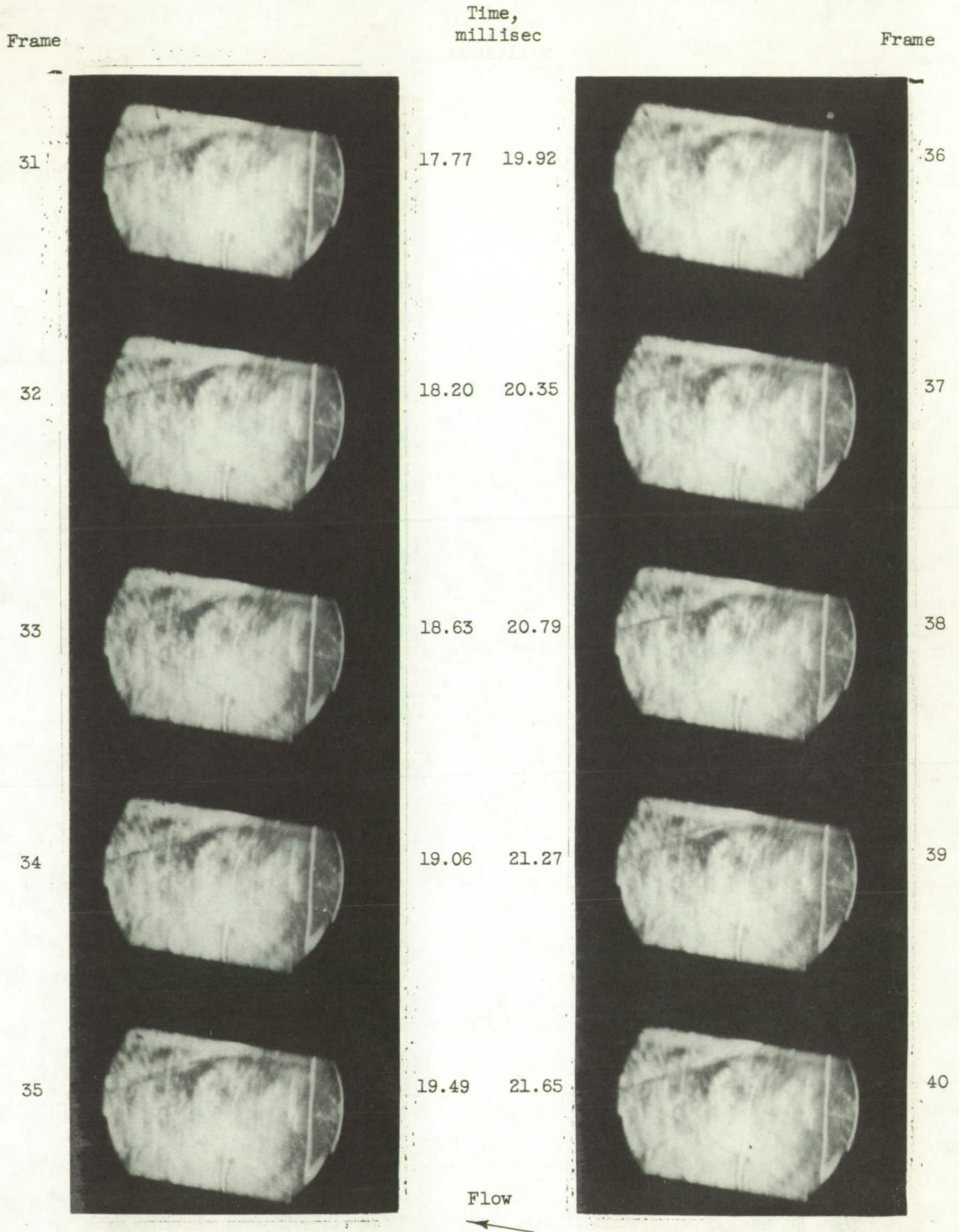
Figure 8. - Continued. Combustion of 1/2-cc aluminum borohydride at Mach 3 (run 25, table III).



C-38248

(b) Continued. Schlieren photographs of tunnel at injection point. Camera speed, 2319 frames per second.

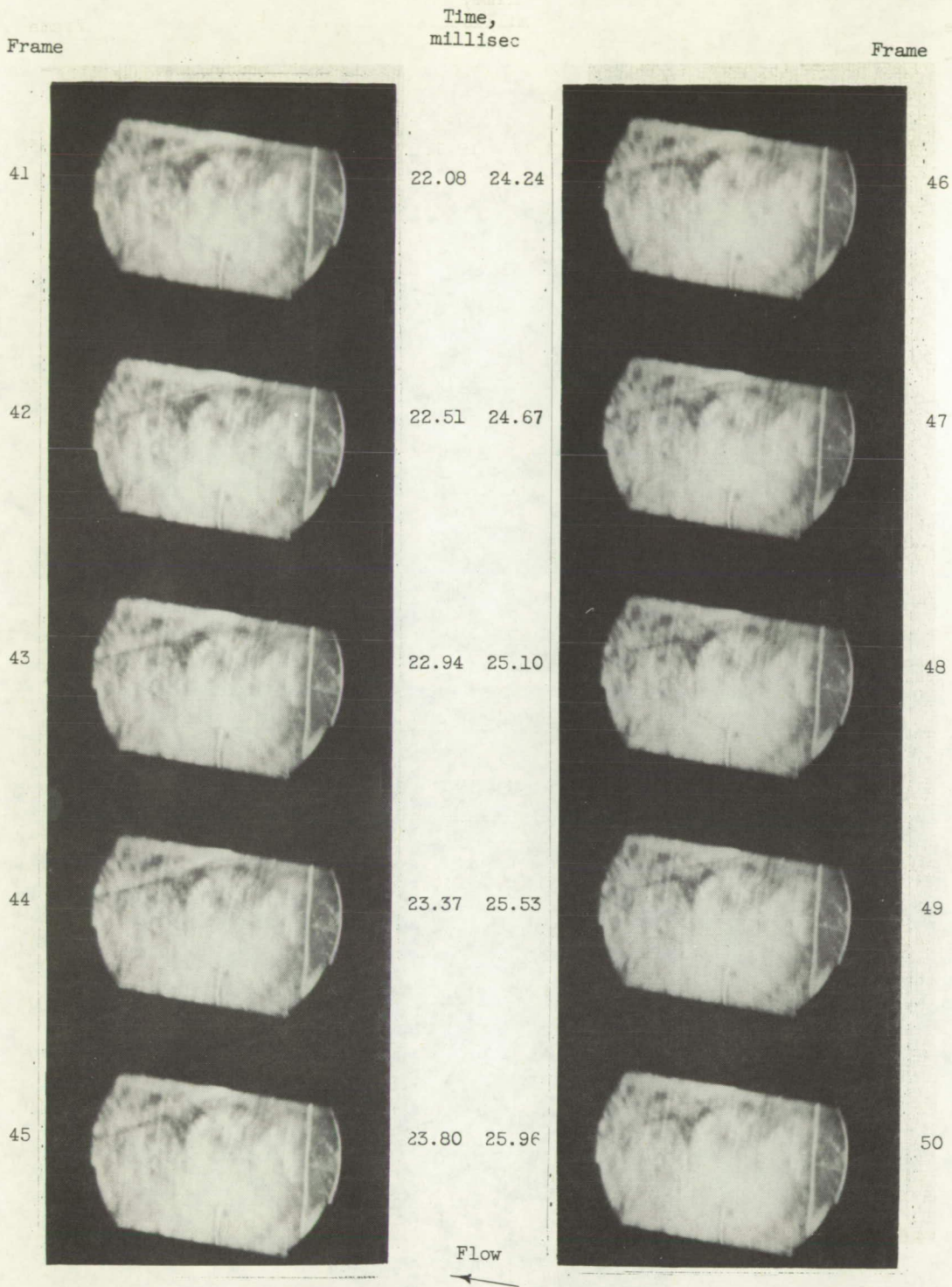
Figure 8. - Continued. Combustion of 1/2-cc aluminum borohydride at Mach 3 (run 25, table III).



C-38249

(b) Continued. Schlieren photographs of tunnel at injection point. Camera speed, 2319 frames per second.

Figure 8. - Continued. Combustion of 1/2-cc aluminum borohydride at Mach 3 (run 25, table III).



C-38250

(b) Concluded. Schlieren photographs of tunnel at injection point. Camera speed, 2319 frames per second.

Figure 8. - Concluded. Combustion of 1/2-cc aluminum borohydride at Mach 3 (run 25, table III).

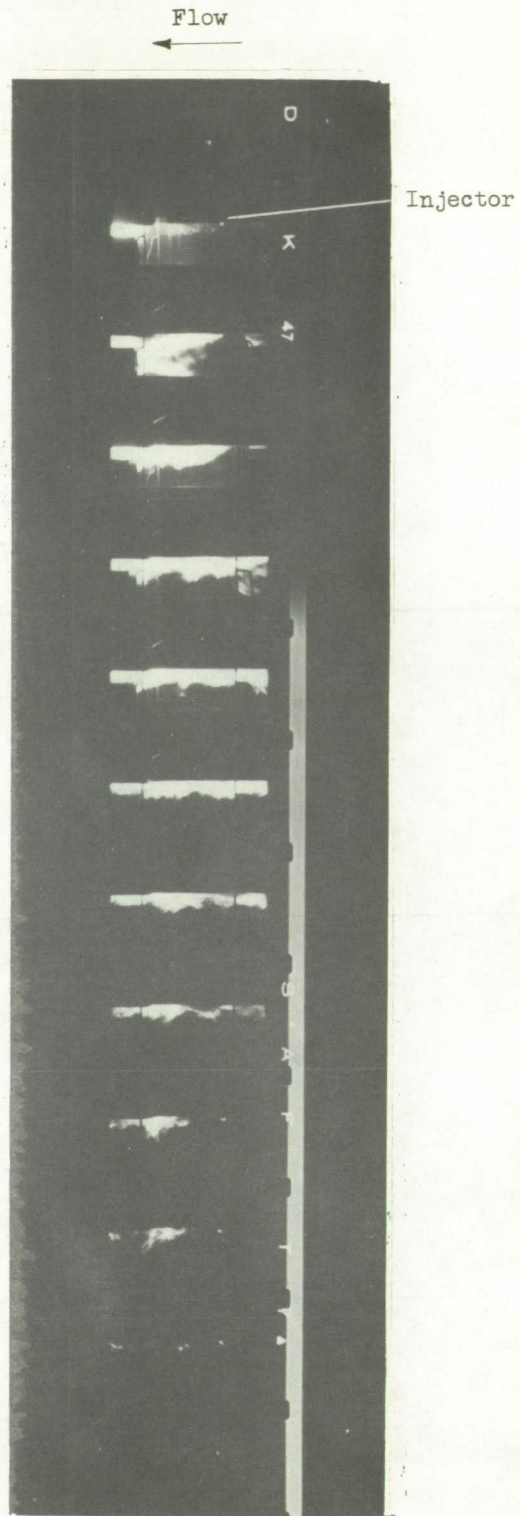
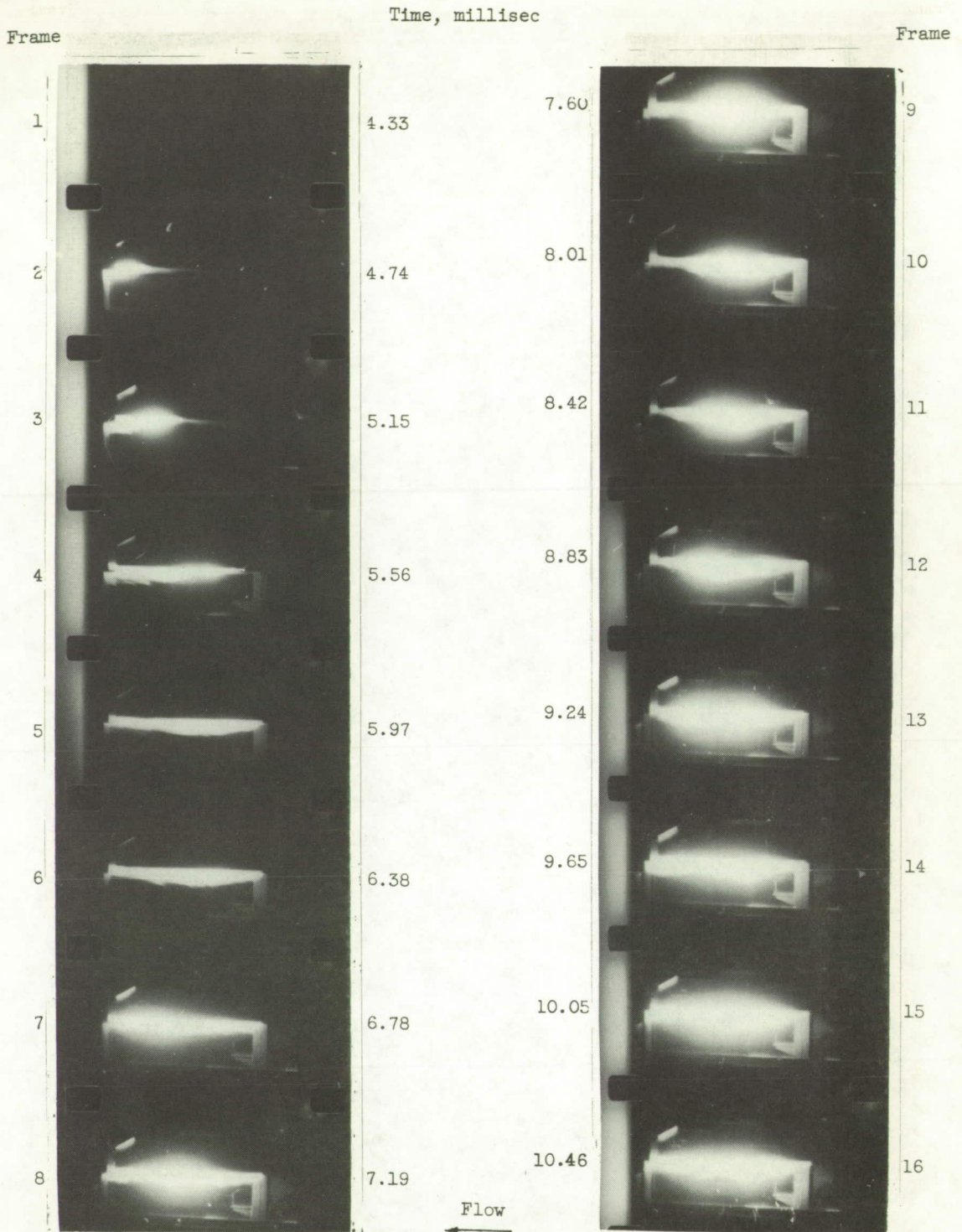


Figure 9. - Explosively violent combustion of 1/2-cc aluminum borohydride at Mach 4 (run 16, table III). Camera speed, 2700 frames per second.



C-56272

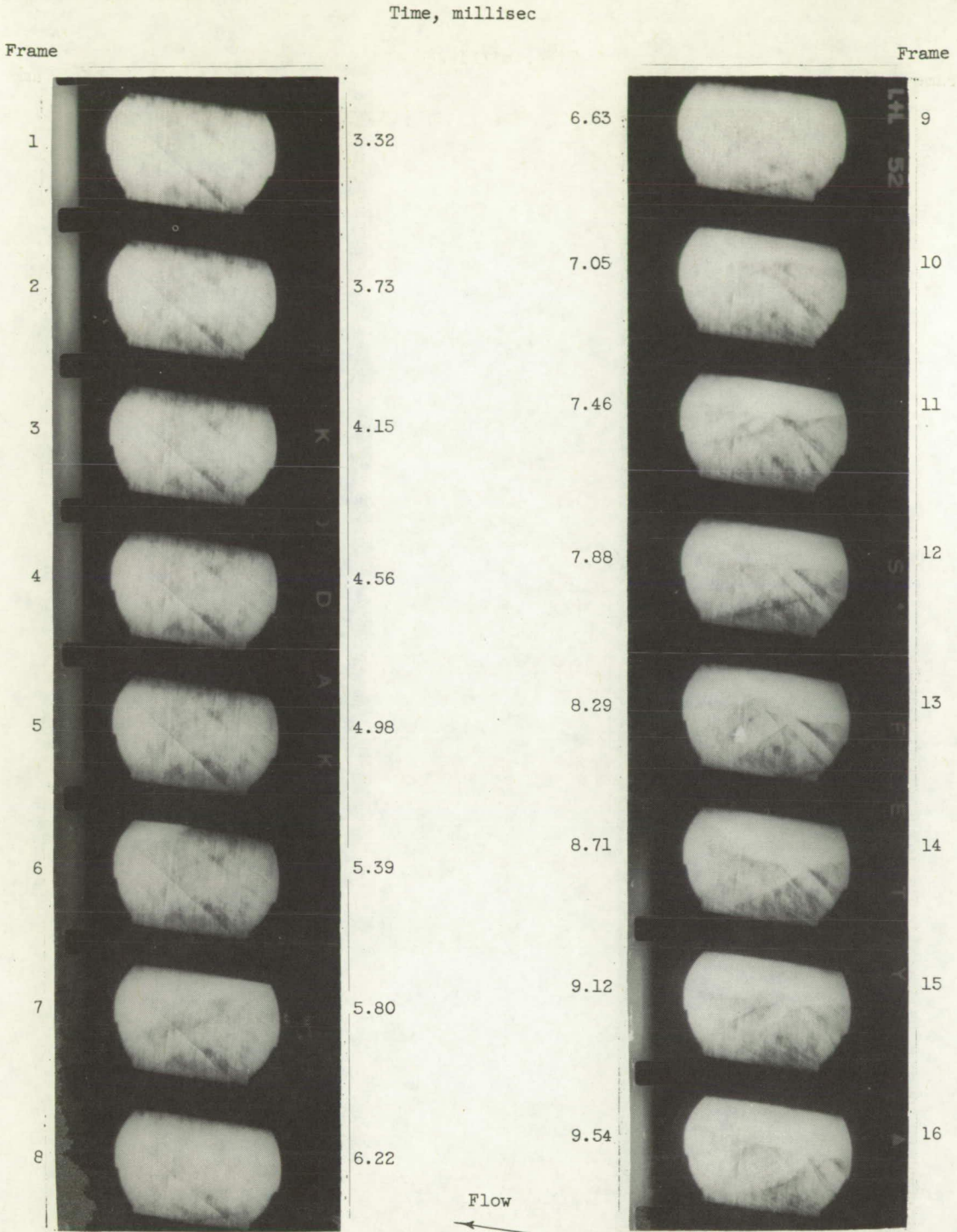
Figure 10. - Open-shutter photograph of combustion of 1/2-cc aluminum borohydride at Mach 4 (run 16 table III). Note that flame extends almost back to throat.



C-38253

(a) Direct motion pictures. Camera speed, 2449 frames per second.

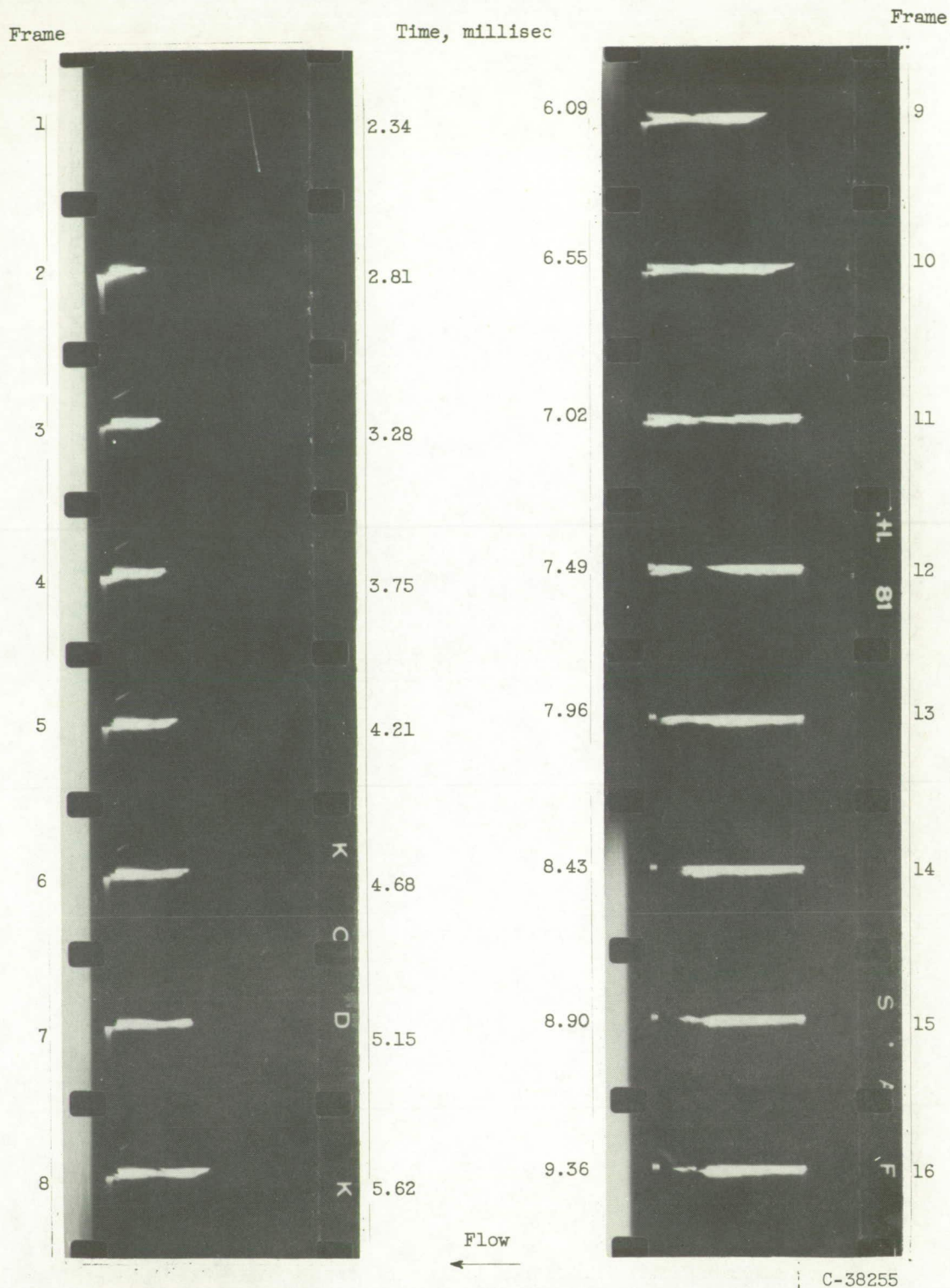
Figure 11. - Early stages of steady combustion of 7-cc aluminum borohydride at Mach 2 (run 7, table IV). Ignition was spontaneous.



C-38254

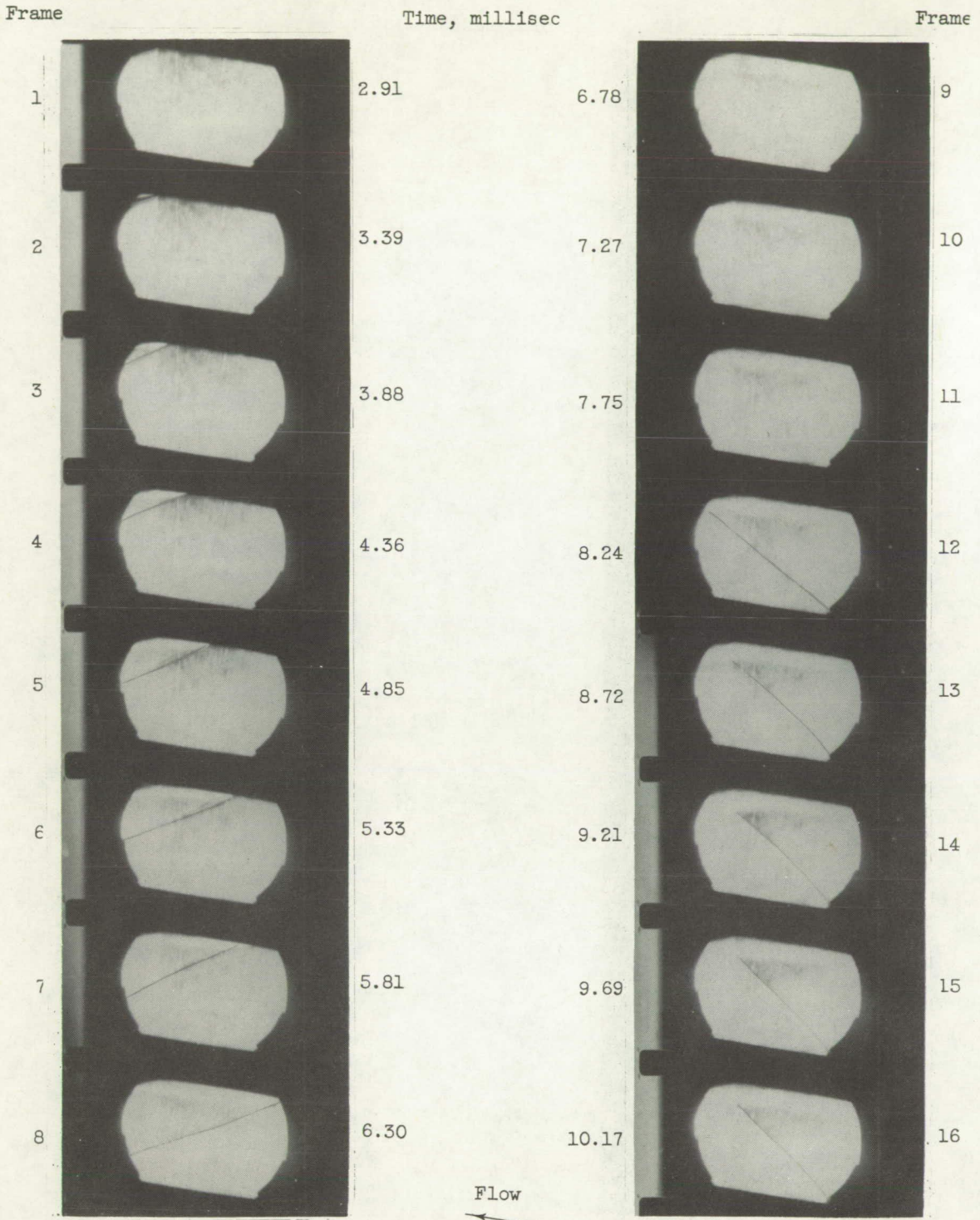
(b) Schlieren photographs. Note lack of shock wave accompanying flame front in frames 6 and following. Center of schlieren system was about 17 inches downstream of injection point. Camera speed, 2412 frames per second.

Figure 11. - Concluded. Early stages of steady combustion of 7-cc aluminum borohydride at Mach 2 (run 7, table IV). Ignition was spontaneous.



(a) Direct motion pictures. Camera speed, 2136 frames per second.

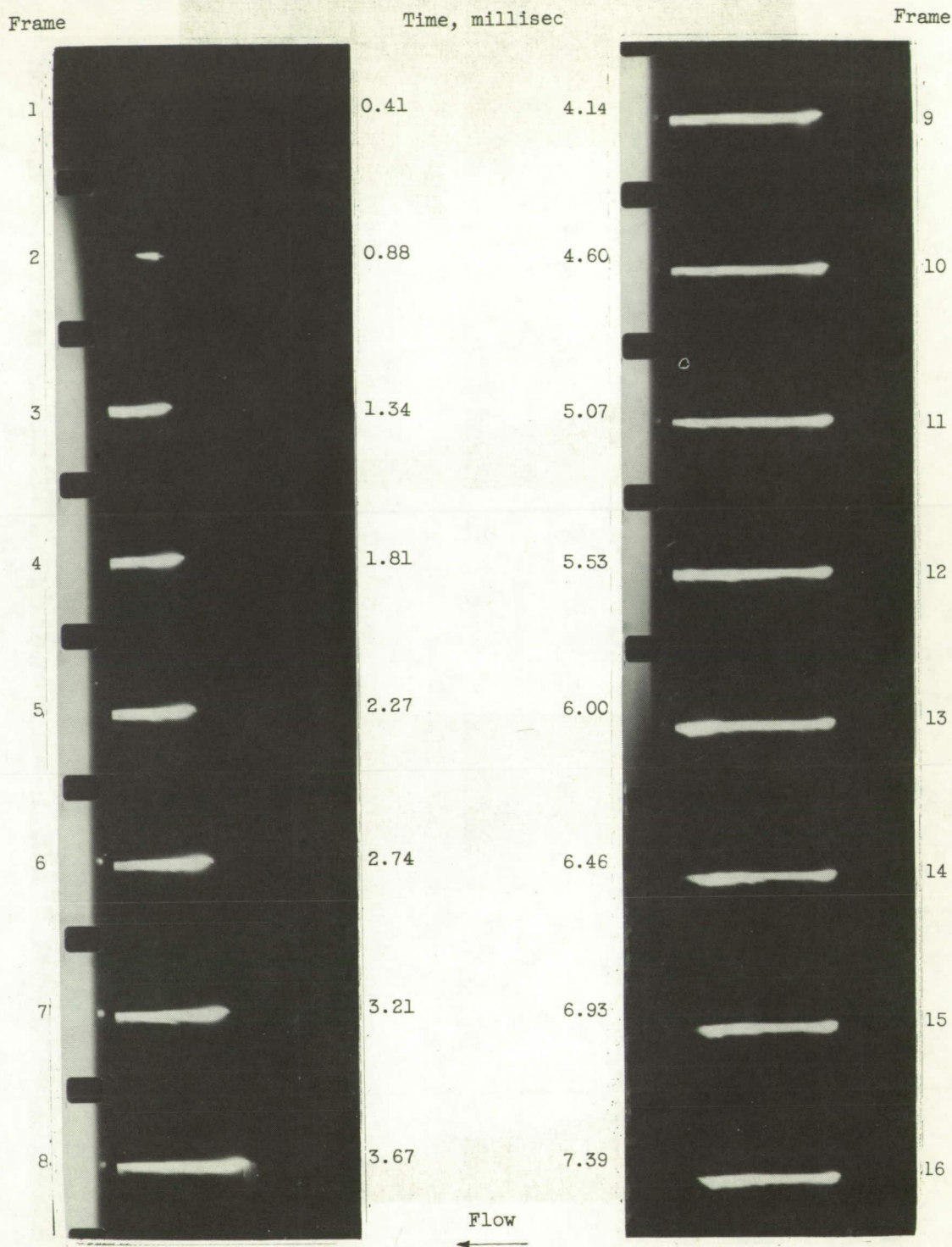
Figure 12. - Steady combustion of 5-cc aluminum borohydride at Mach 2 (run 11, table IV). Ignition achieved by capsule technique.



C-38270

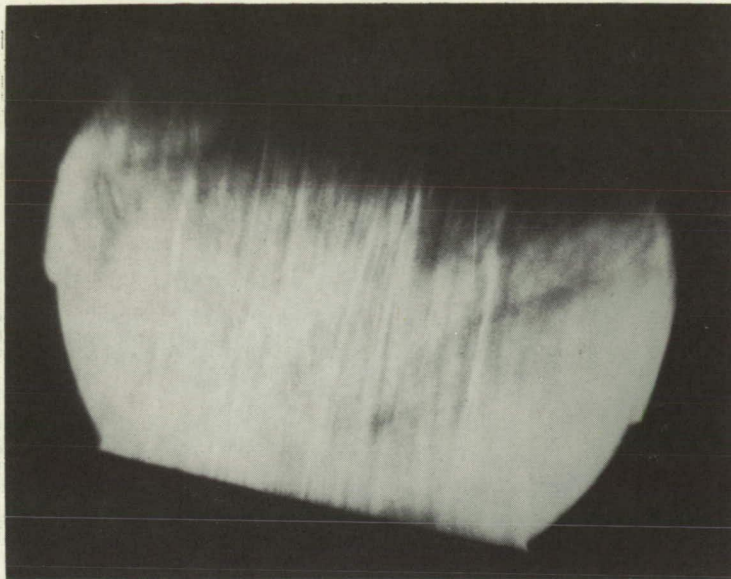
(b) Schlieren photographs. Shock waves retouched. Camera speed, 2064 frames per second.

Figure 12. - Concluded. Steady combustion of 5-cc aluminum borohydride at Mach 2 (run 11, table IV). Ignition achieved by capsule technique.



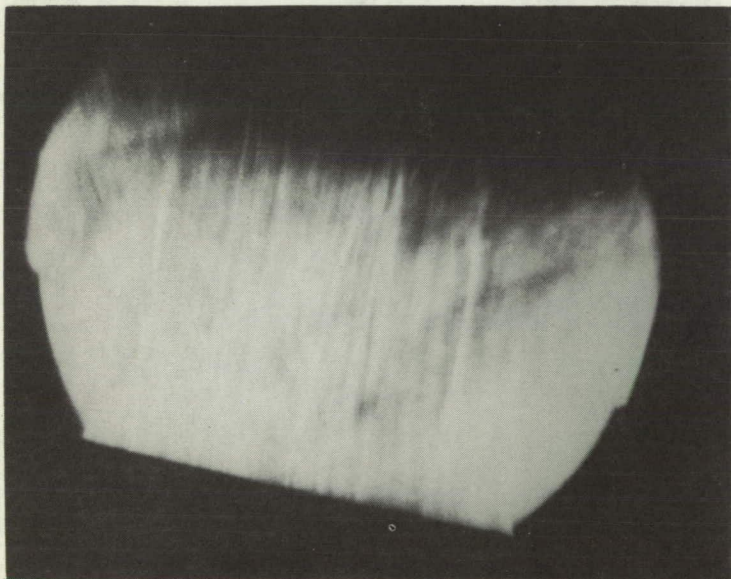
(a) Direct motion pictures. Camera speed, 2149 frames per second.

Figure 13. - Steady combustion of 5-cc aluminum borohydride at Mach 3 (run 18, table IV).



Frame 1; 0.00 millisecc

Flow
←

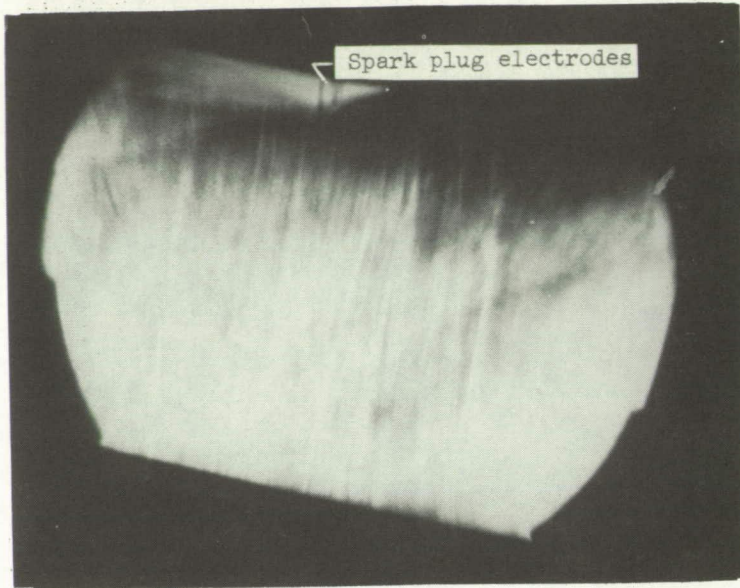


Frame 2; 0.44 millisecc

C-38257

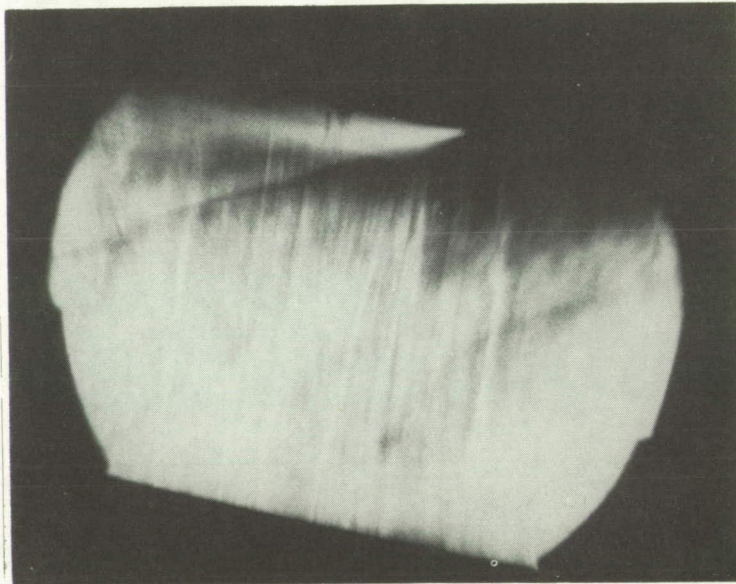
(b) Schlieren photographs at 2280 frames per second, showing ignition at spark plug. Spark-plug electrodes can be seen in frames 3 and following.

Figure 13. - Continued. Steady combustion of 5-cc aluminum borohydride at Mach 3 (run 18, table IV).



Frame 3; 0.88 millisec

Flow

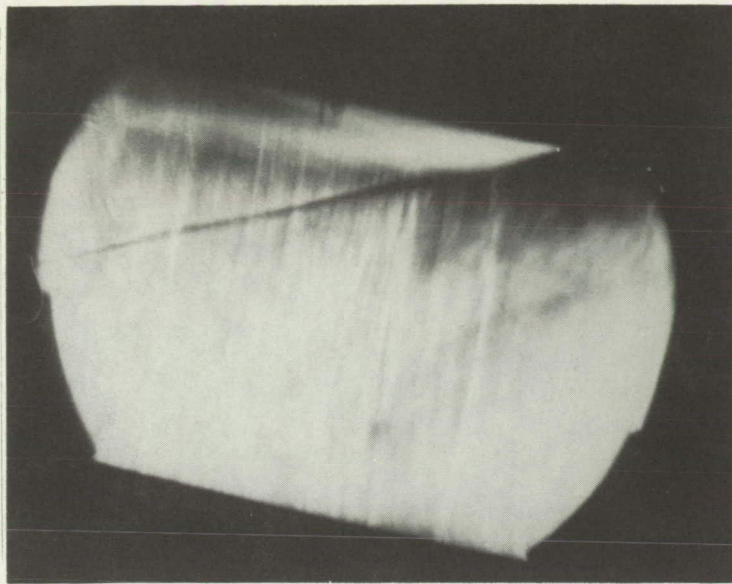


Frame 4; 1.32 millisec

C-38258

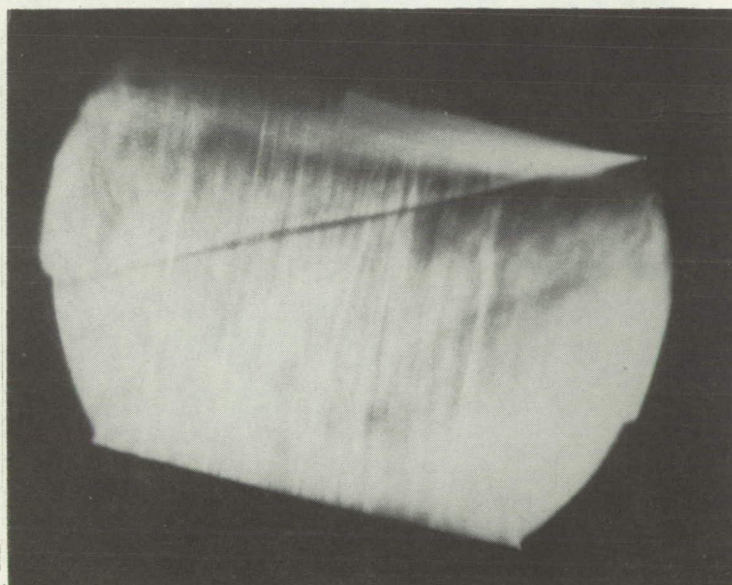
(b) Continued. Schlieren photographs at 2280 frames per second, showing ignition at spark plug. Spark-plug electrodes can be seen in frames 3 and following.

Figure 13. - Continued. Steady combustion of 5-cc aluminum borohydride at Mach 3 (run 18, table IV).



Frame 5; 1.75 millisec

Flow

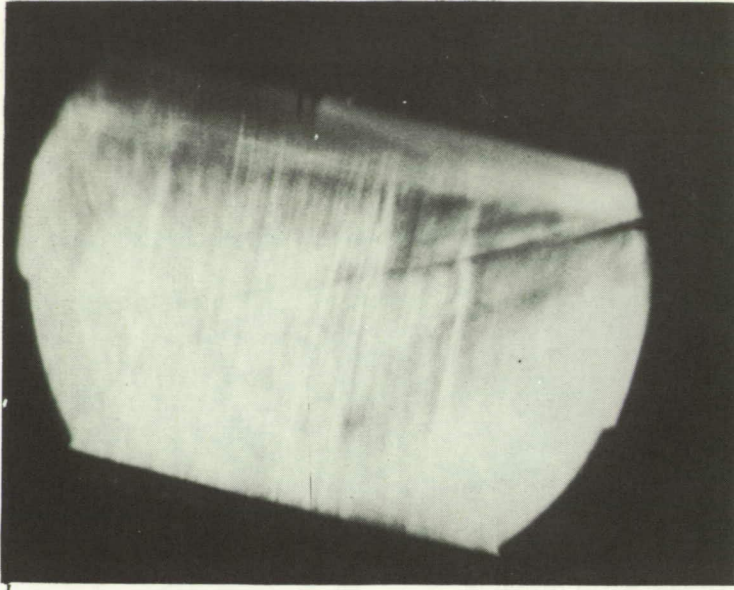


Frame 6; 2.19 millisec

C-38259

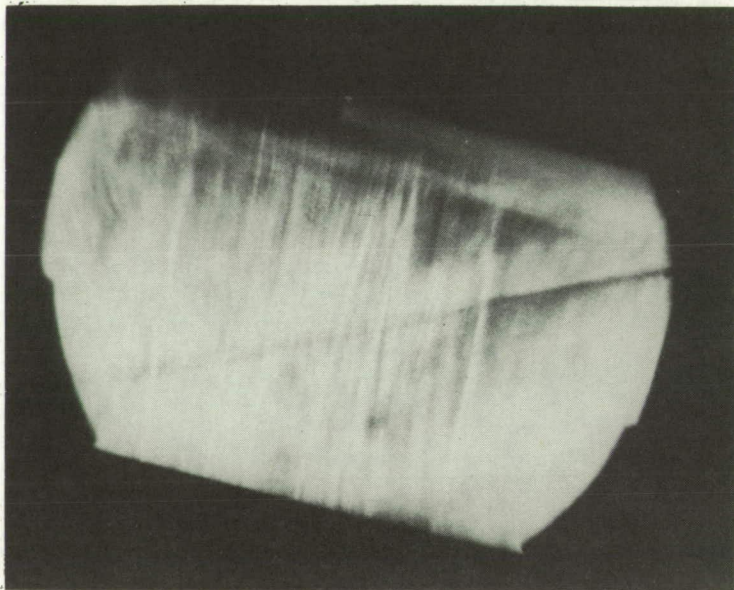
(b) Continued. Schlieren photographs at 2280 frames per second, showing ignition at spark plug. Spark-plug electrodes can be seen in frames 3 and following.

Figure 13. - Continued. Steady combustion of 5-cc aluminum borohydride at Mach 3 (run 18, table IV).



Frame 7; 2.63 millisecc

Flow

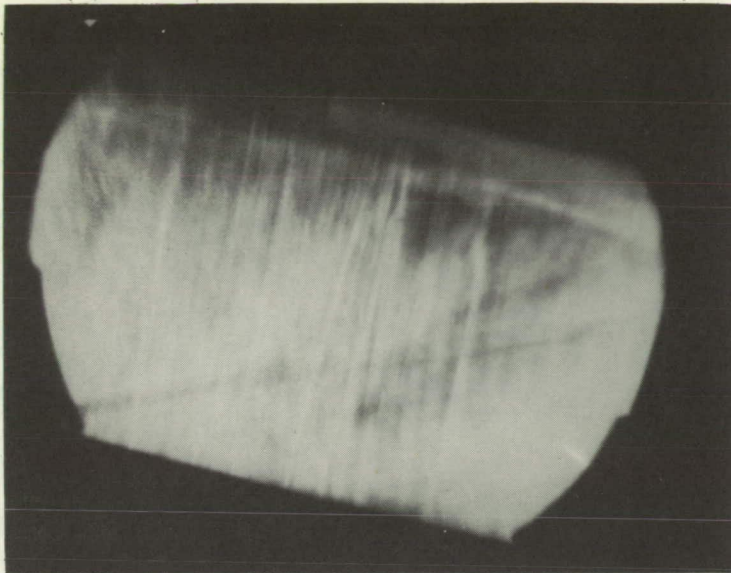


Frame 8; 3.07 millisecc

C-38260

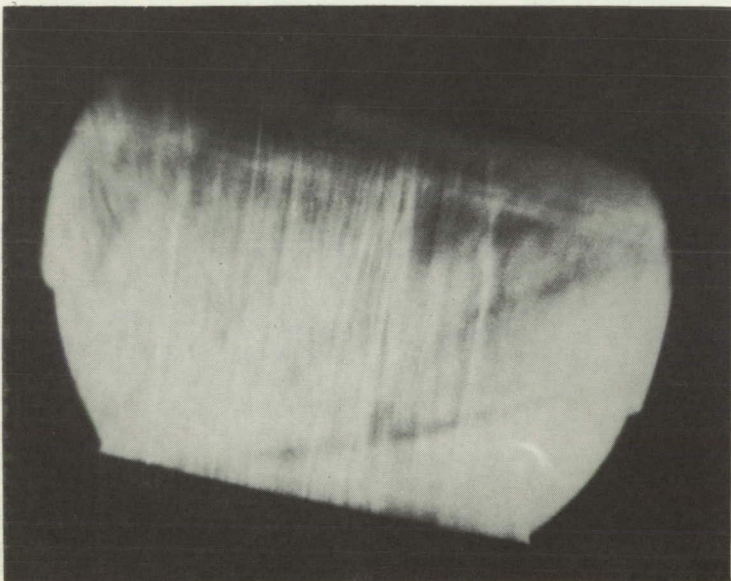
(b) Continued. Schlieren photographs at 2280 frames per second, showing ignition at spark plug. Spark-plug electrodes can be seen in frames 3 and following.

Figure 13. - Continued. Steady combustion of 5-cc aluminum borohydride at Mach 3 (run 18, table IV).



Frame 9; 3.51 millisec

Flow
←

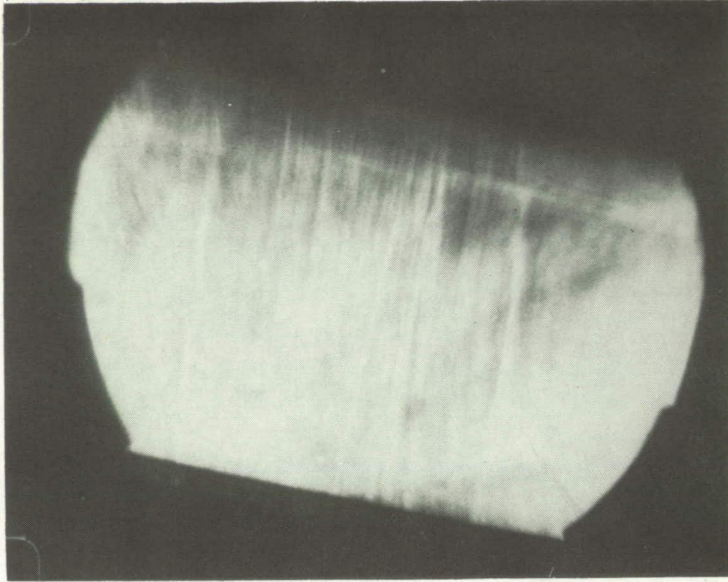


Frame 10; 3.95 millisec

C-38261

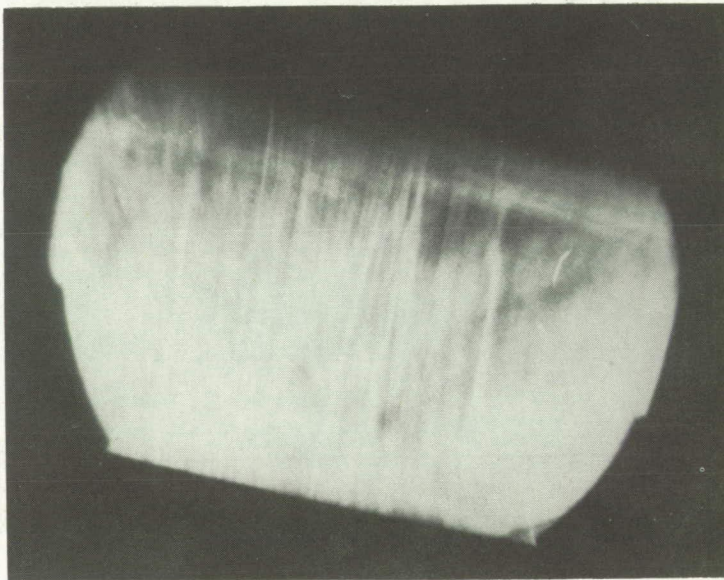
(b) Continued. Schlieren photographs at 2280 frames per second, showing ignition at spark plug. Spark-plug electrodes can be seen in frames 3 and following.

Figure 13. - Continued. Steady combustion of 5-cc aluminum borohydride at Mach 3 (run 18, table IV).



Frame 11; 4.39 millisec

Flow

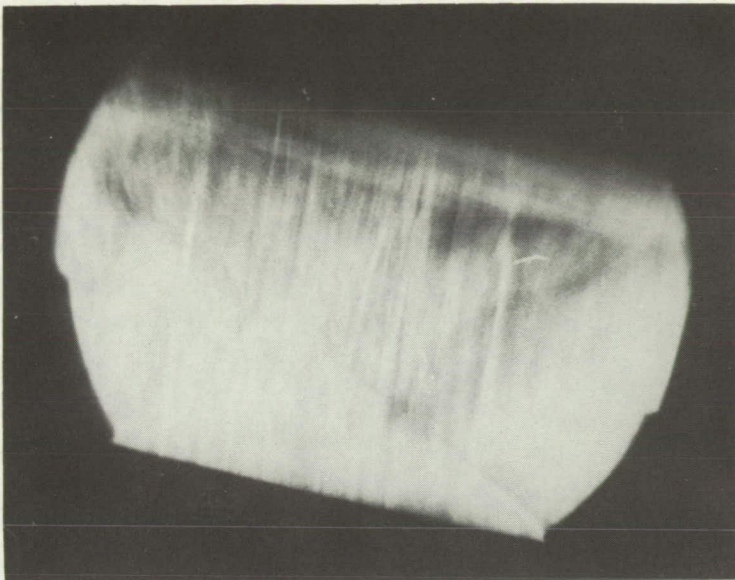


Frame 12; 4.82 millisec

C-38268

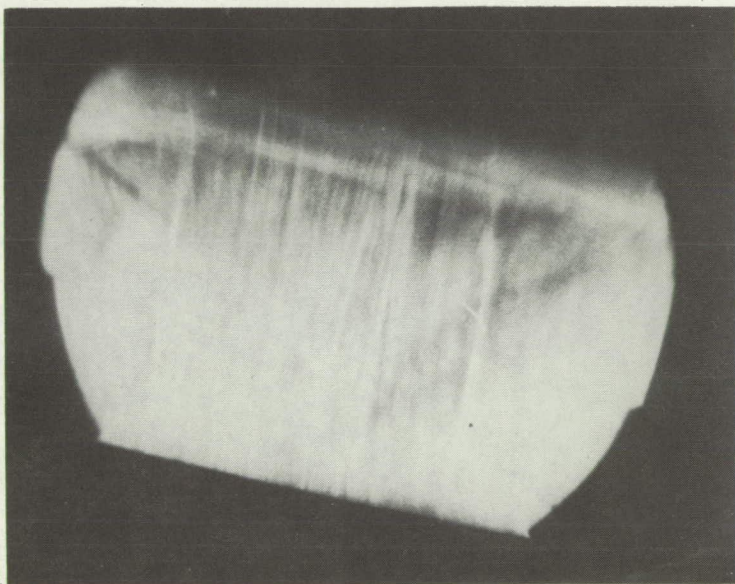
(b) Continued. Schlieren photographs at 2280 frames per second, showing ignition at spark plug. Spark-plug electrodes can be seen in frames 3 and following.

Figure 13. - Continued. Steady combustion of 5-cc aluminum borohydride at Mach 3 (run 18, table IV).



Frame 13; 5.26 millisec

Flow
←

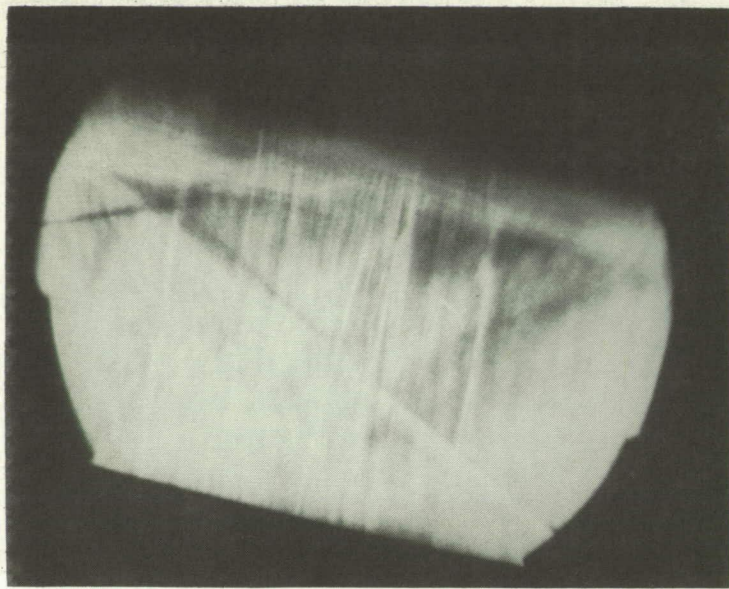


Frame 14; 5.70 millisec

C-38262

(b) Continued. Schlieren photographs at 2280 frames per second, showing initiation at spark plug. Spark-plug electrodes can be seen in frames 3 and following.

Figure 13. - Continued. Steady combustion of 5-cc aluminum borohydride at Mach 3 (run 18, table IV).



Frame 15; 6.14 millisecc

Flow

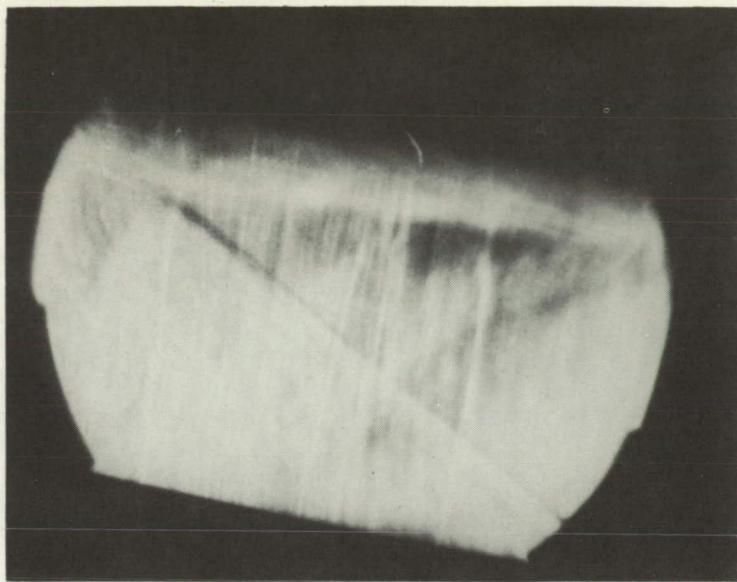


Frame 16; 6.58 millisecc

C-38263

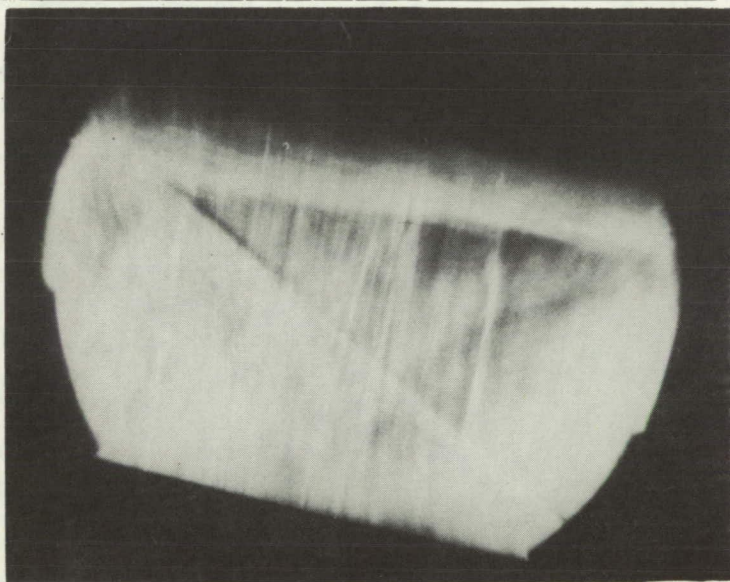
(b) Continued. Schlieren photographs at 2280 frames per second, showing ignition at spark plug. Spark-plug electrodes can be seen in frames 3 and following.

Figure 13. - Continued. Steady combustion of 5-cc aluminum borohydride at Mach 3 (run 18, table IV).



Frame 17; 7.02 millisec

Flow
 ←

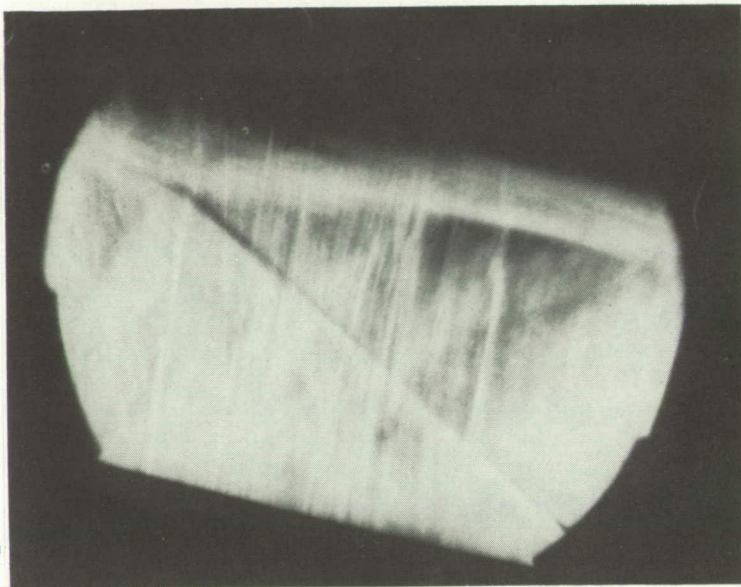


Frame 18; 7.46 millisec

C-38264

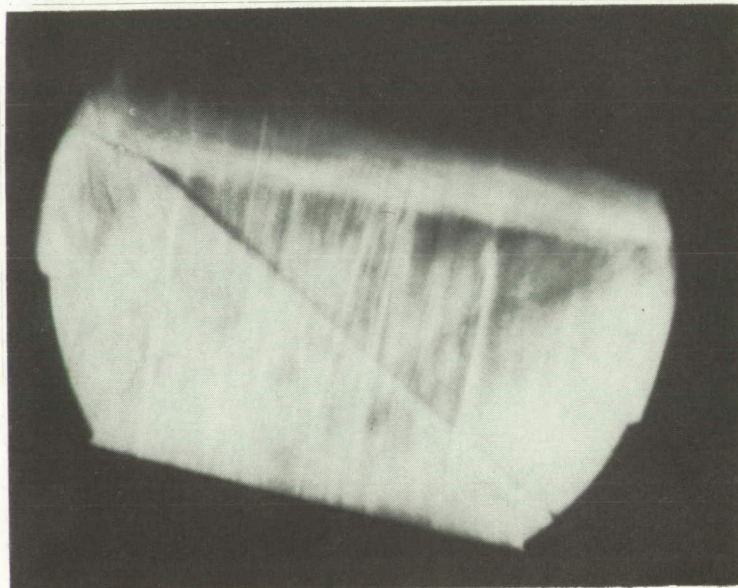
(b) Continued. Schlieren photographs at 2280 frames per second, showing ignition at spark plug. Spark-plug electrodes can be seen in frames 3 and following.

Figure 13. - Continued. Steady combustion of 5-cc aluminum borohydride at Mach 3 (run 18, table IV).



Frame 19; 7.89 millisec

Flow



Frame 20; 8.33 millisec

C-38265

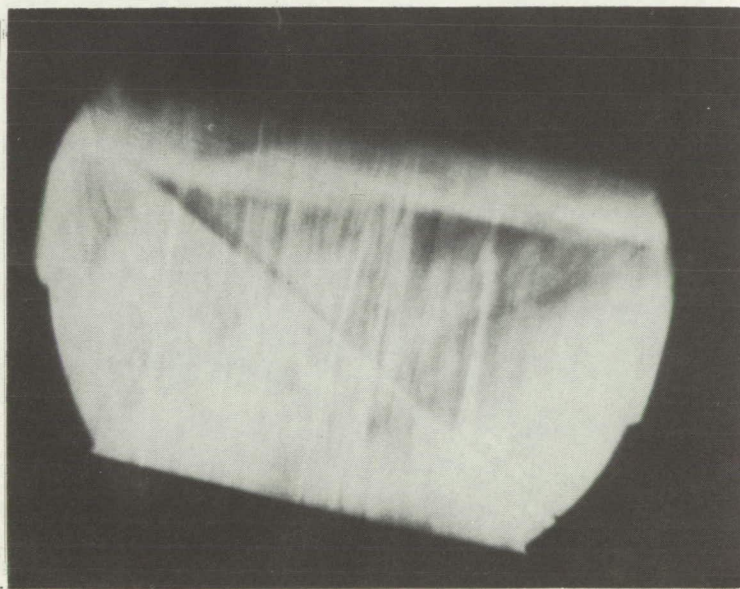
(b) Continued. Schlieren photographs at 2280 frames per second, showing ignition at spark plug. Spark-plug electrodes can be seen in frames 3 and following.

Figure 13. - Continued. Steady combustion of 5-cc aluminum borohydride at Mach 3 (run 18, table IV).



Frame 21; 8.77 millisec

Flow

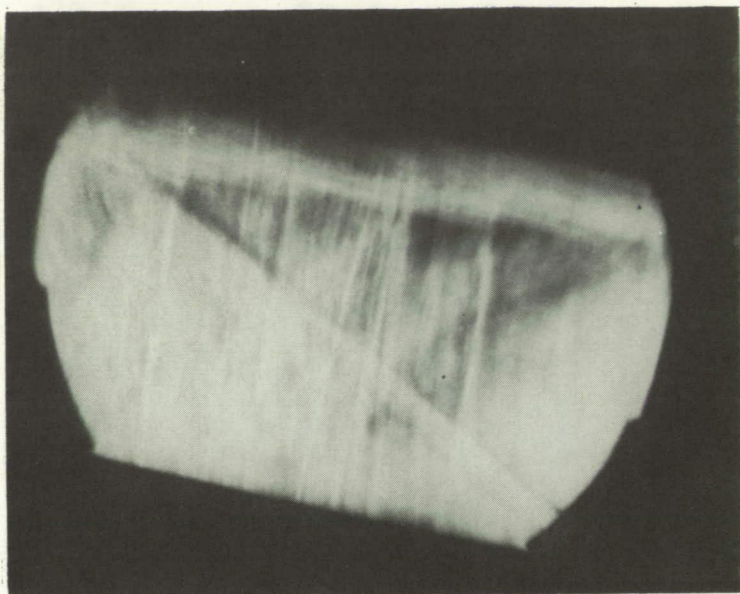


Frame 22; 9.21 millisec

C-38266

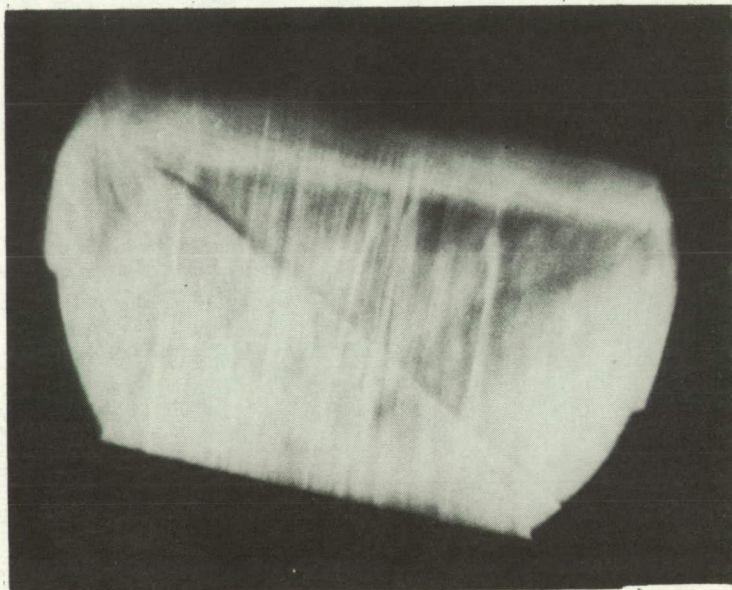
(b) Continued. Schlieren photographs at 2280 frames per second, showing ignition at spark plug. Spark-plug electrodes can be seen in frames 3 and following.

Figure 13. - Continued. Steady combustion of 5-cc aluminum borohydride at Mach 3 (run 18, table IV).



Frame 23; 9.65 millisec

Flow



Frame 24; 10.09 millisec

C-38267

(b) Concluded. Schlieren photographs at 2280 frames per second, showing ignition at spark plug. Spark-plug electrodes can be seen in frames 3 and following.

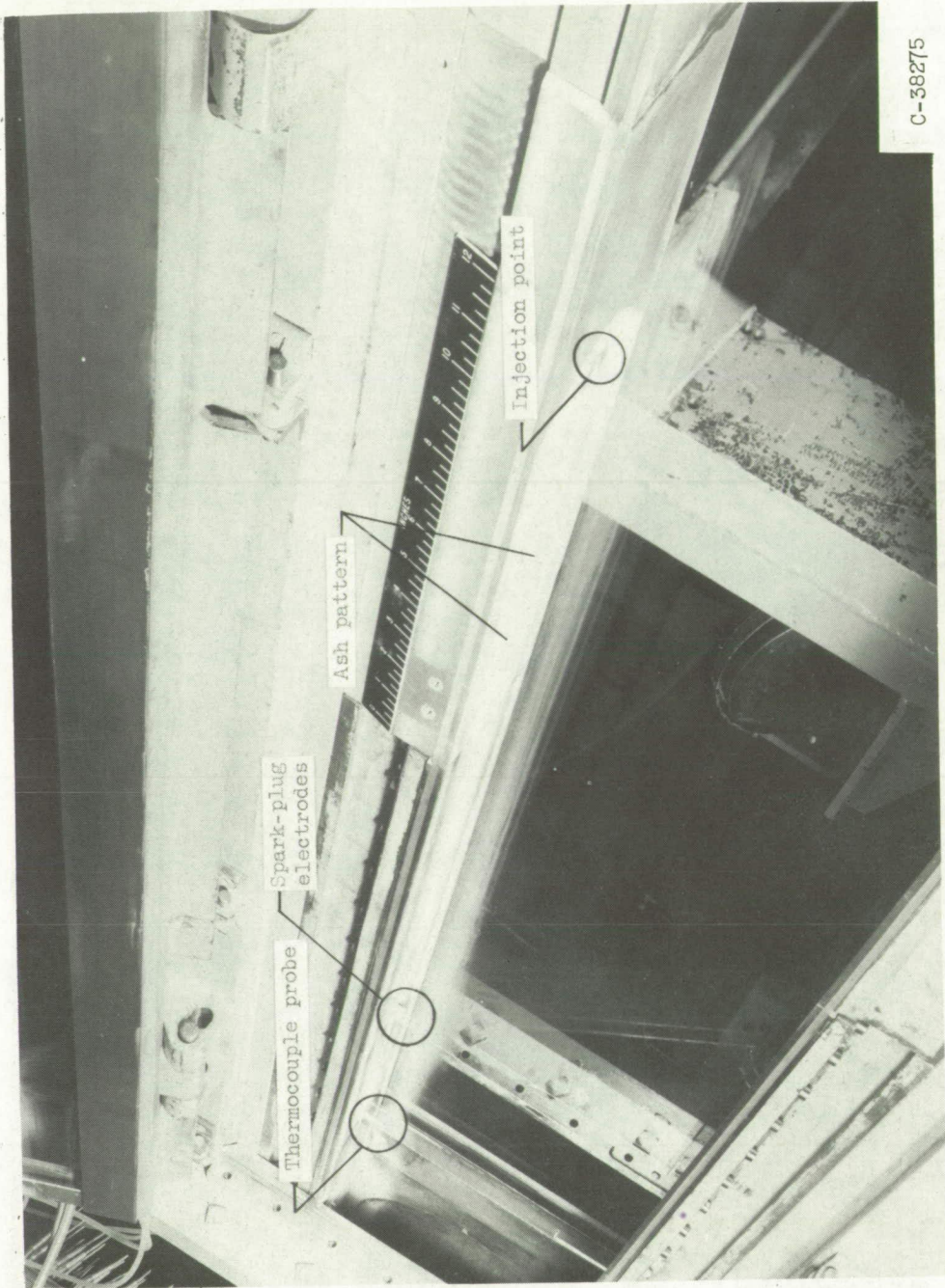
Figure 13. - Concluded. Steady combustion of 5-cc aluminum borohydride at Mach 3 (run 18, table IV).



C-38273

Figure 14. - Open-shutter photograph at Mach 2, showing time-averaged distribution of luminosity associated with steady burning of 5-cc aluminum borohydride (run 13, table IV).

5-25-54



C-58275

Figure 15. - Ash pattern on top wall of tunnel resulting from steady burning of aluminum borohydride at Mach 3. (Ash pattern extends from injection point to end of test section.)